



We are Nitinol.™

## **Overview: Microstructure and Properties of Beta-Titanium**

Duerig, Williams

Beta-Titanium Alloys in the 1980's  
(eds.) R.R. Boyer, H.W. Rosenberg  
pp. 19-69

1984

OVERVIEW: MICROSTRUCTURE AND PROPERTIES OF BETA TITANIUM ALLOYS

T. W. Duerig\* and J. C. Williams\*\*

\*Raychem Corporation  
Menlo Park, CA 94025

\*\*Carnegie-Mellon University  
Pittsburgh, PA 15213  
USA

This paper describes the metallurgical characteristics of  $\beta$ -Ti alloys. Included in this description is a suggested division of this broad class of alloys into lean and rich alloys. A wide variety of phase transformations are possible in these alloys and these are described in general terms. The effects of these transformations on microstructure and properties are also discussed. The effects of processing history on microstructure and properties are also described. Here the differences between lean and rich alloys becomes especially clear. The paper closes with a brief discussion of the authors' view of the outlook for  $\beta$ -Ti alloys.

## 1.0 Introduction

A tremendous variety of phase transformations and attendant property variations have been reported in the Beta Titanium ( $\beta$ -Ti) alloys - far more than in most alloying systems of similar compositional range. Although many of these transformations are still incompletely understood, great strides have been made in the past 10-15 years towards obtaining a sound understanding of these systems. Beta alloys were originally thought to be useful because of the attractive combinations of high strength and toughness that could be uniformly produced through relatively thick cross-sections. This has now been demonstrated for a variety of alloy compositions. More recently, however, researchers have been successful in developing other interesting properties which may come to be of some commercial and practical interest: superelastic properties (1,2,3), superconductive properties (4,5), and shape memory (6,7). In addition, the recognition of excellent hot workability in these alloys may in itself provide sufficient justification to warrant the use of  $\beta$ -Ti alloys in lieu of  $\alpha+\beta$  alloys, irrespective of any potential property benefits (8,9). It is doubtful whether there is any other such narrowly defined range of alloy compositions which is capable of producing such a wide variety of properties. Moreover, such large variations can, in many cases, be observed in a single alloy composition, by simple heat treatment control. For example, in Ti-10-2-3, it has been shown that yield strengths range from 180 MPa (26 ksi) to 1500 MPa (217 ksi), depending upon preceding heat treatments (10). Because of this tremendous variation in properties and microstructures, a detailed understanding of the alloys is complicated, but crucial to their successful application.

Although there are a number of ways one can define the term " $\beta$ -Ti alloy", the following operational definition is generally useful. "A  $\beta$ -Ti alloy is any titanium composition which allows one to quench a very small volume of material into ice water from above the material's  $\beta$ -transus(\*) temperature without martensitically decomposing the  $\beta$ -phase." The point of such a detailed definition is to exclude all Ti alloys in which martensite can be formed athermally or with the assistance of residual stresses which may arise during the quenching of large pieces. It also excludes the diffusional decomposition of  $\beta$  which is section size dependent through cooling rates. The schematic phase diagram (Fig. 1) illustrates the constitution of  $\beta$ -Ti alloys. Within the general class of  $\beta$ -Ti alloys, the solute lean alloys tend to decompose much more readily than do the more stable, solute rich alloys. The properties, and, even more so, the transformations that one finds in the rich and the lean alloys are very different. For the purposes of the following discussion, it is therefore useful to divide the general classification of  $\beta$ -Ti alloys into two sub-classifications: the lean  $\beta$ -Ti alloys, and the rich  $\beta$ -Ti alloys. There is other terminology already embedded in the literature including the terms metastable  $\beta$  and near- $\beta$  alloys. We would argue that these terms are even less precise than those mentioned above. For example, all alloys discussed in this article will decompose to an  $\alpha+\beta$  mixture during aging and thus are metastable. Yet there are wide differences in characteristics within these alloys which our classification system attempts to address. Finally, in view of the foregoing, it is worth mentioning that there are no  $\beta$ -Ti alloys commercially produced in the U.S. which consist of only stable  $\beta$ -phase.

Again there are a variety of ways one can create such a division, but we would propose the formation of isothermal  $\omega$ -phase as the distinguishing

(\*) The  $\beta$ -transus temperature is the lowest temperature at which the equilibrium structure is entirely  $\beta$ ; below the transus, the  $\alpha+\beta$  phases are in equilibrium together.

factor; alloys which form  $\omega$  during aging would be defined as lean alloys, and alloys which are too stable to decompose isothermally to a  $\beta+\omega$  mixture would be classified as rich alloys. Alternatives to this definition would be to define the lean alloys as those which deform by either a twinning or a martensitic shearing process when in the solution treated and quenched condition; or to give a processing oriented definition which would identify the lean alloys as those which can be effectively thermomechanically processed in the  $\alpha+\beta$  phase field (though this definition is certainly the least distinct of the three). In terms of the most common commercial alloys, these three definitions pretty much coincide: any alloy classified as lean or rich by one definition would be classed the same way by either of the other definitions. Nevertheless, one could, without doubt, develop compositions which could not be unambiguously defined by all three definitions, thus we have selected the isothermal formation of  $\omega$ -phase as the distinguishing factor.

Although it is pointless to list and classify all the binary, ternary and higher order  $\beta$ -Ti alloy compositions that have been investigated, it is perhaps useful to see how some of the more important commercial alloys would be divided according to the above definitions. Using any of the three definitions, lean alloys would include the various Transage alloys, Ti-10V-2Fe-3Al\* and Beta-III (11.5Mo-6Zr-4.5Zr). The rich (more stable) alloys would include Ti-8V-8Mo-2Fe-3Al, Ti-15V-3Fe-3Al-3Cr, Beta-C (3Al-8V-6Cr-4Zr-4Mo), and B120 VCA (13V-11Cr-3Al). In terms of the two most common binary systems, the dividing line would seem to be 19-20% Mo, or about 24-25% V. The order in which the alloys are listed above roughly indicates the order of alloy stability, from the leanest, or most unstable alloy (Transage), to the richest (B120 VCA). One should perhaps note that the leanest group of these alloys (the Transage series) may not even be properly classified as  $\beta$ -Ti alloys; it appears as if some Transage compositions form martensite on quenching while others do not (this will be discussed later). In any case, the similarities of both the transformation behavior and the properties of Transage to the other  $\beta$ -Ti alloys makes it entirely proper to include them in the present  $\beta$ -Ti alloy discussion.

With the above sub-divisions, it becomes much easier to make generalizations about  $\beta$ -Ti alloys, and to discuss them in a more coherent way.

## 2.0 Solute Lean $\beta$ -Ti Alloys

Because the lean  $\beta$ -Ti alloys strengthen quite rapidly to very high strengths, they are generally not suitable for use in the  $\beta$  solution treated, quenched and peak aged condition because the strengths are very high and the ductilities and toughnesses typically are too low for most applications. In some cases, extreme over-aging is sufficient to lower strength and to provide acceptable ductility, but in general, solution treatment must be done below the  $\beta$ -transus temperature (termed an  $\alpha+\beta$  solution treatment). The primary effect of such a treatment is to enrich the  $\beta$ -matrix in  $\beta$  stabilizing constituents because Al and Ti are partitioned to the precipitating  $\alpha$ -phase. This increases the stability of the  $\beta$ -phase and reduces its propensity to decompose during subsequent aging; the final aged strength of the alloy is thereby decreased, and the levels of ductility and toughness required in structural applications can be achieved. The usual heat treatment sequence for the lean  $\beta$ -Ti alloys then produces a bimodal distribution of  $\alpha$  in a  $\beta$ -matrix. Coarse, globular  $\alpha$  is produced during the solution treatment, and very fine, acicular  $\alpha$  is precipitated during subsequent aging. These fea-

\*All alloy compositions are given in weight percent unless otherwise specified.

tures are both illustrated in Figure 2. The coarse, globular  $\alpha$  is usually termed ( $\alpha_p$ ) since it is the first  $\alpha$  to appear in the microstructure during processing, and the fine  $\alpha$  is termed secondary, or, more simply, fine  $\alpha$ . With this preview, we will now proceed to discuss the transformations and properties of the lean  $\beta$ -Ti alloys in more detail.

The commercial thermomechanical treatment of  $\beta$ -Ti alloys can be condensed into four steps:

1. Working operations (normally hot rolling or forging)
2. Solution treatment
3. Quenching
4. Aging

Control of all four of these steps is critical to achieving the final microstructures and mechanical properties desired. The format for the following review will be to first discuss the effect of the various processing steps upon microstructures, and then to individually discuss various mechanical properties and how they are affected by these microstructural manipulations. In fact, it will not really be possible to strictly adhere to these guidelines, and some of the more general discussions of properties will have to be presented along with the microstructural review.

## 2.1 Phase Transformations in the Lean $\beta$ -Ti Alloys:

2.1.1 The Effects of Hot Working and Solution Treatment on  $\alpha_p$  and the  $\beta$  Grain Structure. One of the chief differences between the "lean" class of  $\beta$ -Ti alloys and the "rich" alloys is that the latter have lower  $\beta$ -transus temperatures and therefore cannot be extensively worked in the  $\alpha+\beta$  phase field without using extremely high loads. As will be discussed in a later section, concerns related to the formation of continuous grain boundary  $\alpha$  layer tend to preclude solution treatment of the richer alloys below the transus temperature. Lean alloys, on the other hand, can and usually are both worked and solution treated below their transus temperatures in order to maintain the desired distribution, morphology and volume fraction of  $\alpha_p$ . This usually leads to very coarse (on the order of 5-20 $\mu$ m spacing) distribution of globular  $\alpha_p$ , which has little direct effect upon the strength of the alloy but which is nevertheless important for a variety of indirect reasons.

Probably the most important reason for sub-transus solution treatment has already been touched upon: it allows the composition and stability of the  $\beta$ -matrix to be controlled. Heat treatment above the  $\beta$ -transus temperature, a so-called  $\beta$  solution treatment, results in the least stable matrix composition and in the greatest driving force for subsequent decomposition. As the solution treatment temperature is decreased and  $\alpha_p$  is introduced into the structure, the remaining  $\beta$ -matrix becomes enriched in  $\beta$  stabilizing elements and somewhat depleted in Al; this increases the stability of the matrix and reduces the driving force for decomposition during both quenching and aging. As has already been pointed out,  $\alpha_p$  is generally formed at high temperatures and is therefore quite coarse; it contributes little, if anything, to the strength of the alloy. Lower solution treatment temperatures will therefore result in lower strength levels after aging simply because the amount of fine  $\alpha$  that can precipitate after a lower temperature solution treatment is decreased. This is demonstrated for the case of Ti-10-2-3 in Figure 3.

The second important characteristic of  $\alpha_p$  concerns its ability to pin  $\beta$  grain boundaries and reduce their mobility (limiting both recrystallization and grain growth). An example of this is shown in Figure 4. In part (a), a

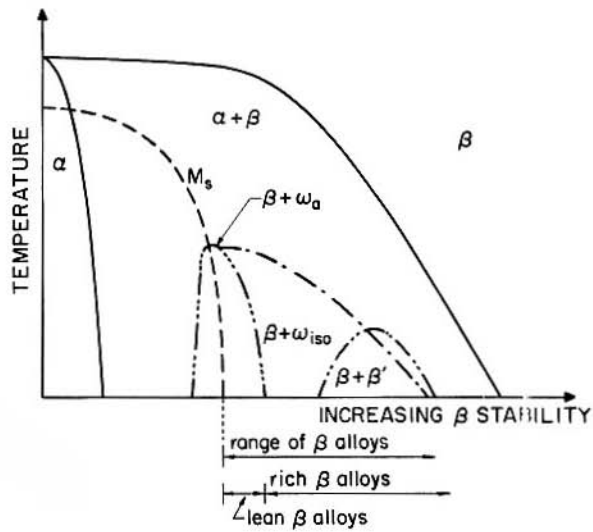


Figure 1. Schematic phase diagram of a  $\beta$ -stabilized titanium system, indicating the compositional range that would be considered  $\beta$  alloys and the subdivision of this range into the "lean" and "rich"  $\beta$  alloys.



Figure 2. Bright field TEM micrograph showing typical bimodal microstructure of a lean  $\beta$  titanium alloy. The coarse, globular primary  $\alpha$  is light colored and monolithic, the fine acicular  $\alpha$  in the surrounding  $\beta$ -matrix is visible only via TEM. This particular microstructure is that of Ti-10-2-3 after  $\alpha + \beta$  solution treating at  $720^\circ\text{C}$  for 2 hrs and then aging at  $400^\circ\text{C}$  for 1000 m.

specimen of 10-2-3 was held at 820°C for 10 minutes; in part (b), a specimen was held for 2 hours at 780°C; and in part (c), a specimen was held further below the transus at 730°C for 72 hours. Above the transus temperature (Fig. 4(a)), recrystallization is extremely rapid, while at 730°C (Fig. 4(c)), there were still no signs of recrystallization after 24 hours at temperature. Recrystallization at temperatures more than 70°C below the transus (Fig. 4(c)), is nearly impossible irrespective of thermomechanical history and the solution treatment time. At intermediate temperatures, (Fig. 4(b)), the density of  $\alpha_p$  particles was insufficient to prevent recrystallization, but was sufficient to limit the final grain size to about 10 $\mu$ m. Thus, proper control of the  $\alpha_p$  distribution provides a means of controlling recrystallization and grain growth, as well as the stability of the matrix itself. One should note, that an increase in aged strength when going from a  $\beta$  solution treatment to an  $\alpha+\beta$  solution treatment is possible because of the finer grain size and greater density of secondary  $\alpha$  nucleation precipitation in the material solution treated below the transus. Thus, the conventional wisdom that lower solution treatment temperatures lead to lower strengths is not without exception. Recrystallization and grain growth are also strongly influenced by the hot working operation. High diffusionaly normalized strain rates (\*) during hot working tend to retard dynamic recrystallization, result in higher internal energies, and increase the tendency of the material to recrystallize during subsequent solution treatment.

We have already said that  $\alpha_p$  has very little direct influence upon the strength of the  $\beta$ -Ti alloys; it does, however, have a direct influence upon fracture phenomenon: toughness and ductility. This influence, which will be reviewed under the heading of mechanical properties, is related to the size, distribution, and morphology of the  $\alpha_p$  particles. Microstructurally speaking, one can summarize the effects of working and solution treatment upon the morphology and size of  $\alpha_p$  as follows:

1. The natural or "free" growth morphology of the  $\alpha$ -phase is high aspect ratio plates, lying on the {110} planes of the  $\beta$ -matrix. Thus  $\alpha_p$  that is precipitated during the solution treatment stage will appear as highly elongated plates (see Fig. 5(a)).
2. If the  $\alpha_p$  phase is then allowed to coarsen during solution treatment, it will begin to spheroidize (the plate geometry is favored due to kinetic reasons, not due to equilibrium energy considerations) An example is shown in Figure 5(b)). This process is not very rapid, however, because the plate morphology is reasonably stable.
3. The geometry and distribution of  $\alpha_p$  present during the hot working operations is governed by still other considerations. Extensive hot working in the  $\alpha+\beta$  phase field tends to break up the  $\alpha_p$ , leading to a finer  $\alpha$  distribution, of a more equiaxed morphology (11).
4. Extremely heavy reductions during working in the  $\alpha+\beta$  region will tend to elongate the  $\alpha_p$  in the directions of maximum material flow, so again a plate-like geometry can be produced, though now the plates are not crystallographically aligned (illustrated in Fig. 5(c)). Thus, structure is unstable and recrystallizes during subsequent annealing.
5. Finally, there is always a tendency to precipitate  $\alpha$  on the grain boundaries. If  $\alpha$  is allowed to precipitate freely (during a solution treatment),

(\*)This is defined as strain rate divided by the diffusivity. This parameter increases by either reducing the temperature of hot working, or by increasing the strain rate.

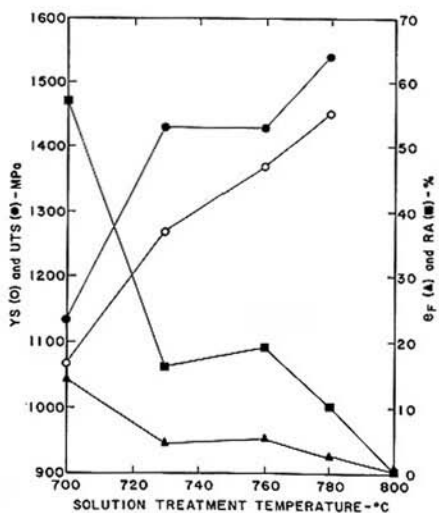


Figure 3. Yield strength, ultimate tensile strength, reduction in area, and elongation of Ti-10-2-3 after solution treating for 8 hrs at various temperatures and aging at 500°C for 60 m.

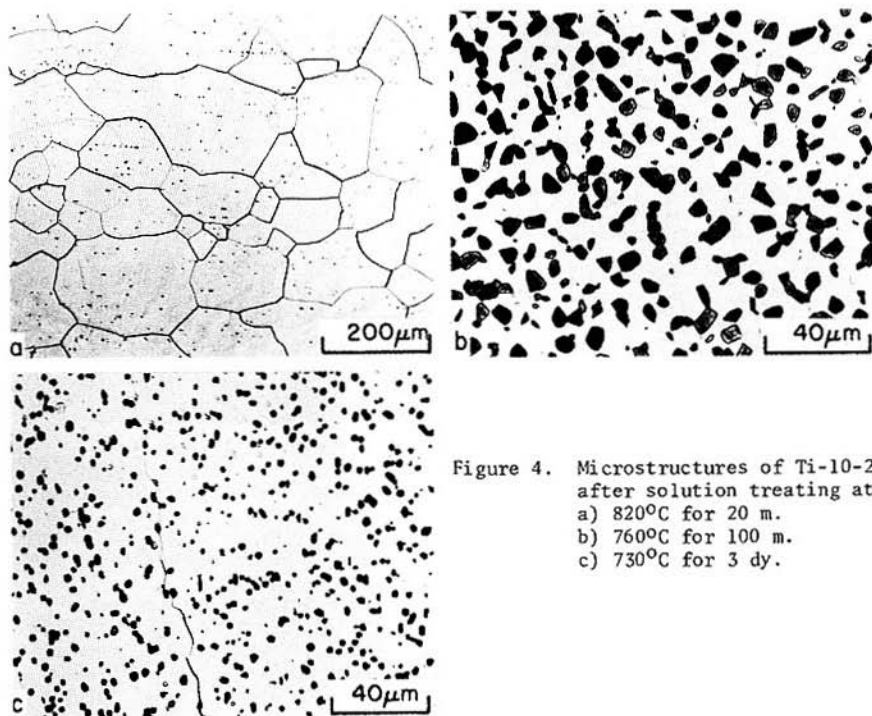


Figure 4. Microstructures of Ti-10-2-3 after solution treating at:  
 a) 820°C for 20 m.  
 b) 760°C for 100 m.  
 c) 730°C for 3 dy.



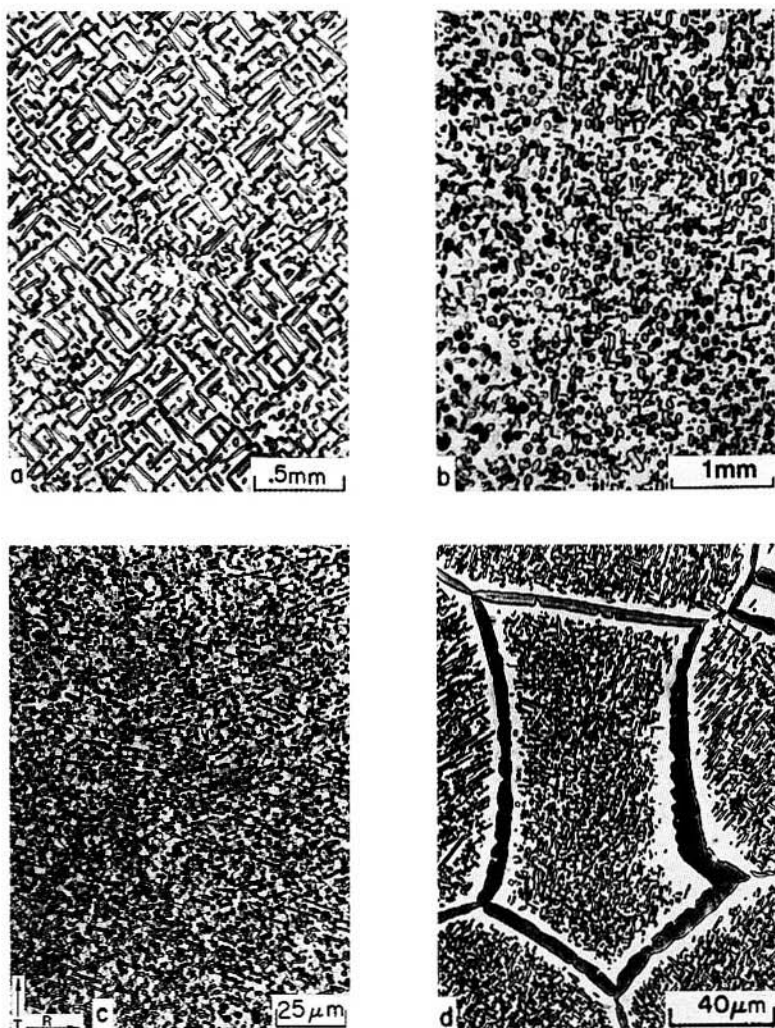


Figure 5. Four types and/or morphologies of primary  $\alpha$ : a) crystallographically elongated, b) equiaxed, c) deformed, and d) grain boundary.

it will be preferentially precipitated on the grain boundaries, often forming a continuous grain boundary  $\alpha$  layer (Fig. 5(d)). This microstructural constituent is always detrimental to ductility and often to toughness. In fact, because of the strong tendency for grain boundary  $\alpha$  formation, these alloys cannot be worked and then  $\alpha+\beta$  solution treated. In these alloys, solution treatment should be used to modify the  $\alpha_p$  distribution by growing or shrinking the existing  $\alpha_p$  introduced during hot working, but should not be done in a way which precipitates new particles because many of these will form along grain boundaries.

From the above points one can deduce that the finest grain sizes are obtained by low hot working temperatures relative to the  $\beta$ -transus and by solution treating very close to the  $\beta$ -transus temperature; this prevents dynamic recrystallization, provides a high driving force for subsequent recrystallization (thus forcing recrystallization despite the pinning effect of the  $\alpha_p$  during the sub-transus solution treatment), and then prevents the recrystallized grains from growing rapidly. It should, however, be noted that very low solution treatment temperatures have been reported to lead to inhomogeneous grain size distributions, and that there exists a "window" for optimum hot working (12). A duplex solution treatment technique has also been used in Ti-10-2-3 (11,13). The treatment consists of a first solution treatment very close to the  $\beta$ -transus temperature, a slow cool, and then a second treatment some 10°C below the first. The strategy behind this approach is reportedly to obtain elongated  $\alpha_p$  during the first treatment, and then to introduce new  $\alpha_p$  of a more equiaxed nature during the second. It seems doubtful, however, that a second treatment only 10°C lower than the first would introduce any new  $\alpha$ , but that it would instead grow the  $\alpha_p$  remaining from the first. Furthermore, it is difficult to imagine why the second treatment would produce  $\alpha$  which is more equiaxed than the first. Other microstructural studies (14) have not verified that the final  $\alpha$ -phase distribution resulting from such a duplex treatment is any different than results from a simple one-step treatment at the temperature of the final duplex treatment. If a difference in properties does exist, it would seem more logical to attribute it to recrystallization because the first treatment is high enough to allow recrystallization while maintaining a fine grain size; the second treatment simply normalizes the volume fraction of  $\alpha_p$  to the volume fraction which corresponds to the final solution treatment temperature. As a final comment, the optimum heat treatment of the Transage alloys has been reported to consist of the following three-step process: a  $\beta$  solution treatment, an initial aging treatment close to the transus, which could be called an  $\alpha+\beta$  solution treatment, then a second aging treatment at lower temperatures (15). Micrographs, however, do show evidence of grain boundary  $\alpha$  layer after such treatments, so it may simply be that the optimum thermo-mechanical sequence has not yet been identified.

2.1.2  $\beta$ -Phase Decomposition During Quenching: Athermal  $\omega$  and  $\alpha''$  Martensite. There are two types of quenching transformations that have been observed in the lean  $\beta$ -Ti alloys: athermal  $\omega$ -phase ( $\omega_a$ ) and the  $\alpha''$  martensite. Although neither transformation is particularly effective in strengthening the  $\beta$ -matrix, both phases have significant effects upon subsequent precipitation hardening events, and in this respect are quite important.

The mechanics of the athermal  $\beta \rightarrow \omega$  transformation have been discussed and reviewed extensively in the last 15 years (16-21), and will only be briefly summarized here. The formation of  $\omega$ -phase occurs by a diffusionless, or compositionally invariant transformation that requires only very small atomic shuffles (similar to a martensitic transformation). These shuffles consist of periodic compressions of the  $\{111\}_\beta$  along the  $\langle 111 \rangle$  which is normal to each of these planes. The wave-like nature of these displacements is some-

what analogous to spinodal decomposition, except that displacement waves are involved instead of compositional waves. The  $\omega_a$  precipitates have hexagonal (or nearly hexagonal) symmetry, with a c/a ratio of only 0.633, and a packing efficiency equal to that of the BCC structure. The particles are fully coherent with the  $\beta$ -matrix, are very fine (on the order of 1-3 $\mu$ m), and have no obvious or distinct shape (see Fig. 6). The physical appearance of discrete  $\omega$  particles is accompanied by diffuse streaking in X-ray and electron diffraction patterns. This streaking results from sheets of diffuse intensity which form an octagon bounded by the  $\langle 111 \rangle$  planes of the reciprocal BCC lattice and can actually precede the actual formation of discrete  $\omega$  reflections and particles. Streaking, therefore, can be found in the richer alloys as well as the lean alloys, and should not in itself be considered conclusive proof of the presence of  $\omega$ -phase. Although hydrostatic pressures can be used to produce rather high volume fractions of  $\omega$ -phase (22), the volume fractions of  $\omega_a$  found at atmospheric pressures are always lower and the particles are small and closely spaced, thus the effect of  $\omega$  on the as-quenched properties is generally quite small. Practical interest in  $\omega_a$  stems only from its influence upon subsequent precipitation sequences, and possibly from its competition with the martensitic decomposition process (i.e., the formation of  $\omega_a$  during quenching may prevent martensitic decomposition)(23).

Although a variety of different martensitic crystal structures have been reported in Ti alloys, recent evidence indicates that only two are found in bulk specimens: the hexagonal  $\alpha'$ , and the orthorhombic  $\alpha''$ . In fact,  $\alpha''$  is simply a slightly distorted hexagonal structure, with the same atomic positions as the hexagonal structure, but distorted so that the lattice has lattice parameters between those of the BCC  $\beta$ -matrix and those of the hexagonal  $\alpha'$  structures (23,24) - a compromise between the two. This point is illustrated in Figure 7, in which both the BCC and HCP lattices are redefined as orthorhombic lattices. This viewpoint is consistent with and supported by the Burger's orientation relationship which describes the orientations of  $\alpha$  and  $\alpha'$  with the  $\beta$ -matrix:

$$\begin{array}{l} (110)_\beta \parallel (0001)_\alpha \\ [111]_\beta \parallel [11\bar{2}0]_\alpha \end{array}$$

If one were to describe the same crystallographic relationship in terms of the orthorhombic systems outlined in Figure 7, one would arrive at the following self-consistent relation, where p and m represent parent and martensite, respectively:

$$\begin{array}{l} (001)_p \parallel (001)_m \\ [\bar{1}10]_p \parallel [\bar{1}10]_m \end{array}$$

The relationship of  $\alpha''$  with the  $\beta$  lattice can be described by the same relation, substituting  $\alpha''$  for  $\alpha'$  (with a two degree rotation required to produce the observed habit). Thus, one can gain substantial insight into the martensitic transformation by viewing both the body-centered cubic and hexagonal structures as special cases of the orthorhombic structure. As one might expect, the orthorhombic parameters become nearer to those of the BCC structure as the  $\beta$  stability of the alloy is increased (25-28). Hammond has proposed that the orthorhombic distortion is introduced to accommodate interstitials (29). There is no experimental evidence, however, to support this supposition, and it is not clear how it would tie into the fact that increasing the  $\beta$  stabilizer concentration leads to an increasing orthorhombic distortion.

There are two ways methods of obtaining martensite in Ti alloys: by quenching (athermal martensite), and by applying an external stress (stress-

induced martensite). There also is a correlation between the structure of the martensite and its mode of formation. The  $\alpha'$  can form either athermally or as a stress assisted product but  $\alpha'$  only forms athermally. Some alloy compositions (Transage (30), Ti-10-2-3 (23), and Ti-6-2-4-6 (31), for example) exhibit both types of transformation: some martensite forms athermally, but the application of an external stress induces even more. We will now address some observations concerning the formation of martensite during quenching. Although the martensite is structurally identical to that formed by a stress-induced process, the particulars of the stress-assistance process will be separately discussed in a later section.

The observation of quenching martensite in alloys like Ti-10-2-3 and Transage may at first seem contradictory to the definition of " $\beta$ -Ti alloys" offered earlier, but this is not necessarily the case. For one, it is fairly clear that quenching stresses can provide sufficient stress to trigger a stress-induced transformation in certain compositions (10,23). Large specimens, when quenched, appear martensitic, while very thin specimens of the same material undergo no transformation. Similarly oil quenched specimens may not undergo transformation, while water quenched specimens do. In any case, the definition of a  $\beta$ -Ti alloy offered above carefully excluded all compositions that transform as a result of quenching stresses. These residual quenching stresses are not the only artifacts confusing the identification of quenched microstructures in the lean  $\beta$ -Ti alloys. It is already well-known that microstructural characterization via TEM is difficult due to transformations induced by thin-foil relaxation (32,33). It is also evident that simple mechanical polishing can be sufficient to induce a thin surface martensite layer. To avoid this, both optical and X-ray specimens should be electropolished. Although X-ray diffraction patterns obtained from electropolished surfaces should provide clear evidence with respect to the presence of martensite, this evidence is not always unambiguous with regard to the structure of the martensite. To dependably distinguish between the hexagonal and orthorhombic martensites, one must look at more than one crystal orientation; many of the more convenient testing geometries (such as with the beam direction perpendicular to rolling plane) often mask all of the distinguishing orthorhombic peaks (such as the  $(1\ 2\ 0)$ ), and even a highly distorted orthorhombic structure can be improperly identified as hexagonal; this has been verified in both Transage alloys (34) and in Ti-Mo binaries (35). There is still one more complicating issue. The Ms temperature-composition curve on a Ti phase diagram tends to be very steep, or even vertical at temperatures below  $\sim 400^\circ\text{C}$ . As a result, it becomes essentially correct to speak in terms of an Ms composition - that is, a composition separating martensitic alloys from non-martensitic alloys. Alloys with nominal compositions very near this critical value could, in fact, fluctuate from one side to the other, depending upon local variations in chemistries and heat-to-heat variations.

Although it may not be easy to predict, or even to identify the presence of martensite in the as-quenched structure, martensite does play an important role in the subsequent aging response of the material. (This will be illustrated in Figure 12). It is, therefore, relevant to take a closer look at stability of some commercial alloys relative to the Ms line. Of the more important lean commercial alloys, only Beta III is clearly too stable to ever form martensite upon cooling; all of the richer  $\beta$ -Ti alloys are, of course, too stable to decompose as well. Ti-10-2-3 would seem to lie just to the right of the Ms line, though one can apparently go to the left of the line and still stay within the bounds of the nominal compositional specifications (36). The case of the Transage alloys is the least clear. Optical microstructures have been published showing no martensite whatsoever (37), and showing a largely transformed matrix (30). Crossley (37-39) has said

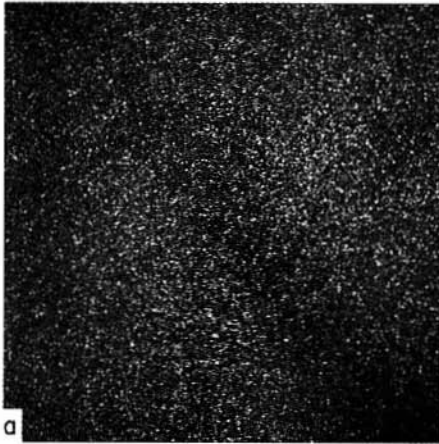
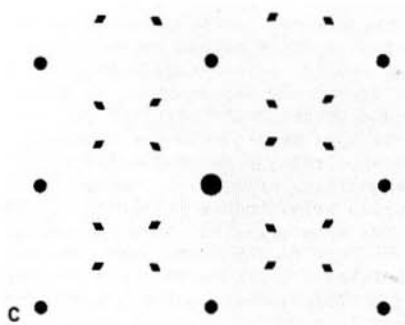
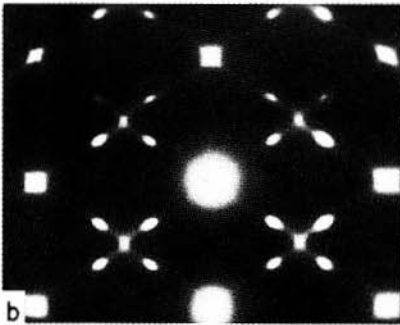


Figure 6. Typical TEM evidence of athermal  $\omega$ -phase:  
 a) DF micrograph taken with  $\omega$  reflection,  
 b) typical electron diffraction pattern of  $[110]_{\beta}$  zone showing both  $\beta$  and  $\omega$  reflections,  
 c) indexed schematic of (b) where diamonds are  $\omega$ -reflections from two different crystallographic variants.



that martensite is present, but is "sub-microscopic" and present in such low volume fractions that it cannot be detected via X-ray diffraction, only by TEM. However, this point of view does not reflect the particular difficulties associated with thin-foil relaxation as mentioned earlier. Other X-ray investigations have shown that martensite forms in some ingots and not in others, suggesting that the nominal compositional range includes the Ms line (40). However, in no case was evidence found for "sub-microscopic" martensite. Considering all the experimental difficulties mentioned above, we feel that X-ray diffraction should be considered the final determinate as to whether or not an alloy is martensitic. On this basis, we feel that Transage alloys are very similar to Ti-10-2-3 in terms of stability to martensitic decomposition.

**2.1.3 Stress-Induced Martensite and Shape Memory.** Transage alloys, Ti-10-2-3, and a variety of binary systems have been shown to undergo a stress-induced martensitic transformation in the quenched and unaged (or underaged (7) condition). The transformation is most evident in a tensile test (Fig. 8). At stress levels as low as 150 MPa, the  $\beta$ -phase begins to undergo a transformation to  $\alpha''$ . The  $\alpha''$  transformation accommodates the applied load by producing a tensile strain. After some 3-4% strain, the transformational strain is exhausted and the stress begins to rise again. This second rise goes on uninterrupted until the proper dislocation flow stress is reached. In the case of Ti-10-2-3, the transformation process has been shown to be accompanied by mechanical twinning. It is also interesting to note that the stress needed to induce the martensitic transformation does not appear to reach a minimum at the Ms temperature, as it does in most other thermoelastic systems (41); it instead begins to increase quite sharply at temperatures well above Ms. Although the reason for this is not entirely clear, it has been proposed that there is a competition between the athermal  $\beta \rightarrow \omega$  transformation and the  $\alpha''$  transformation. This might also explain why the Ms line is so steep in these alloys.

In many alloys too rich to exhibit these martensitic transformations, deformation can take place by mechanical twinning. This has been studied in Ti-V (42,43), in Ti-Mn (44), and in Beta-III (45). Two twinning systems have been observed:  $\{3\ 3\ 2\}\langle 1\ 1\ 3\rangle$  and  $\{1\ 1\ 2\}\langle 1\ 1\ 1\rangle$ . The  $\{3\ 3\ 2\}\langle 1\ 1\ 3\rangle$  twinning systems is somewhat uncommon in bcc metals. It has been proposed that the  $\{3\ 3\ 2\}\langle 1\ 1\ 3\rangle$  system is compatible with the  $\omega$ -phase structure, and therefore favored in  $\beta+\omega$  matrices (45). There are inconsistencies in this reasoning, however, since the  $\{1\ 1\ 2\}\langle 1\ 1\ 1\rangle$  twinning system has been observed in other  $\omega$ -phase containing systems (14,46).

In alloys that exhibit the stress-induced martensitic transformation, the original, pre-deformation shape can be restored in some of these alloys by heating the material rapidly back to its  $A_s$ -temperature.  $A_s$  has only been accurately measured in two alloys: Ti-10-2-3 (6) and Ti-45%Nb (7), and in both cases,  $A_s$  was reported to be approximately 200°C. The magnitude of this shape memory effect has been shown to depend upon the heating rate and the magnitude of original deformation (Fig. 9), with the maximum recovery being on the order of 4%. There are four interesting features of these shape memory observations:

1. Shape memory effects of this magnitude were at one time thought not to exist in disordered alloys (47,48). (The reasoning for the ordering requirement was that ordering would force the martensite to revert to the original  $\beta$ -phase variant in preference to creating anti-phase boundaries).

2. Shape memory recoveries above 200°C are very unusual.

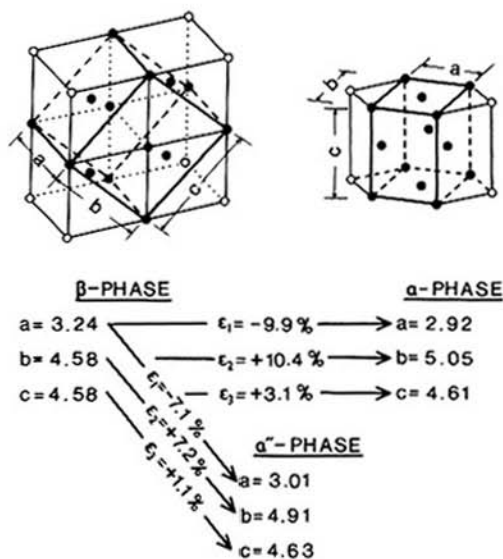


Figure 7. An illustration of how the lattices of the  $\alpha$ ,  $\beta$ , and  $\alpha'$  phases are interrelated. Also shown are the transformation strains for  $\beta \rightarrow \alpha'$  and  $\beta \rightarrow \alpha$  transformations.

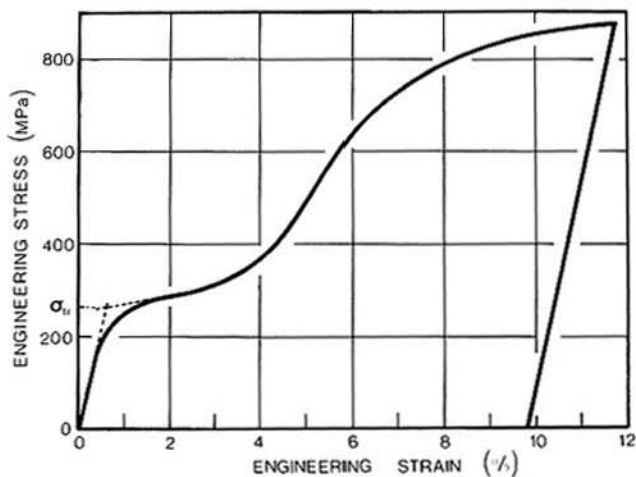


Figure 8. Stress-strain curve of  $\beta$ -solution treated and quenched Ti-10-2-3; deformation behavior is controlled by the stress-induced  $\beta \rightarrow \alpha'$  transformation.



3. The hysteresises of the martensite transformation in both  $\beta$ -Ti alloys and in other disordered memory systems (e.g., FeMn (49)) are extremely large: often greater than 200°C. The reason for this apparent trend is not clear, but deserves further study.

4. The observation of shape memory is strong, or even conclusive proof that the transformation is, in fact, stress-induced, and not plastic strain induced.

5. The existence of shape memory would seem to imply that the lattice invariant shear mechanism is one of twinning, as has been suggested by Blackburn and Williams (50), and not slip as has been reported elsewhere (51). Confirmation of this by TEM has been of limited success due to the relaxation effects mentioned earlier.

The shape memory effect in  $\beta$ -Ti alloys exhibits two properties of seemingly great commercial importance: the large hysteresis and the high transformation temperatures. Unfortunately, these alloys are unstable above  $A_s$  and tend to rapidly decompose to a  $\beta+\omega$  mixture. It is not clear if this instability could be eliminated, but this would seem to be a critical step towards taking commercial advantage of the shape memory effect.

2.1.4  $\beta$  Decomposition: The Precipitation of  $\omega$ -Phase. Aging any of the "lean" alloys at low temperatures (up to approximately 400°C, depending upon the specific alloy composition) results in the precipitation of isothermal  $\omega$ -phase. This type of  $\omega$ -phase can be distinguished from the athermal  $\omega$ -phase discussed above because it forms only upon aging, it is larger in size, and there is a composition gradient across the  $\beta$ - $\omega$  boundary. Specific observations of the  $\omega$ -phase structure in commercial compositions include Ti-10-2-3 (16), Transage 134 (30,52), Beta-III (53) and Ti-15Mo-5Zr (54). It now appears as if the formation of isothermal  $\omega$ -phase in these lean alloys is simply a continuation of the athermal  $\omega$ -phase transformation - after the  $\omega$  structure is formed,  $\beta$ -stabilizing elements are continuously rejected from the  $\omega$ -phase particle during aging, and the particles are stabilized (16). Because of the compositionally invariant way in which  $\omega$ -phase particles can grow, the physical growth process of the  $\omega$  structure can be quite a bit faster than compositional stabilization. This sequence is supported by the observation of morphological changes during continued aging (indicative of misfit changes) (16), as well as by the observation that  $\omega$ -phase is suppressed by direct aging (i.e., quenching directly to the aging temperature) (55). Omega particles can be found in two distinct morphologies (56-58): cuboids (found in high misfit systems such as Ti-V, Ti-Cr, or TiFe), and ellipsoids (found in low misfit systems such as Ti-Mo and TiNb, and in high misfit systems during the early stages of solute segregation). In addition,  $\omega$ -phase seems to take on a non-descript shape, reminiscent of athermal  $\omega$ -phase, during the early stages of low temperature aging. Particle sizes as large as 0.2 microns have been observed (59), and still there has been no loss of coherency reported. Unlike the two quenching transformations, isothermal  $\omega$ -phase has a drastic effect on the mechanical properties of the alloy. These effects are discussed in a subsequent paper within this same volume in fair detail (60), and will be briefly summarized in the mechanical property section of this review.

2.1.5  $\beta$  Decomposition: The Precipitation of  $\alpha$ -Phase. Nearly all commercial components made from Ti alloys are processed to produce a fine  $\alpha+\beta$  dispersion. Both the  $\beta$  and  $\alpha$  phases are by themselves quite soft; the relative strengths of the two phases in a given alloy, depends very much on the nominal alloy composition and on the particular heat treatment. Nevertheless, a  $\beta$ - $\alpha$  interface is still an effective hinderance to dislocation movement and



can therefore be an effective matrix strengthener when the  $\alpha$ -phase precipitates are finely enough dispersed. The varieties of  $\alpha$ -phase found in  $\beta$ -Ti alloys share many attributes with the  $\alpha$ -phase in the  $\alpha+\beta$  alloys. Like the  $\alpha+\beta$  alloys, two types of  $\alpha$ -phase have been reported; that which obeys the Burger's orientation relation (called Burger's or Type I  $\alpha$ ), and  $\alpha$ -phase which does not seem to obey that relation, but is instead oriented in a complex and incompletely understood manner (called non-Burger's  $\alpha$ , or Type II  $\alpha$ (\*)). One of the most obvious differences between the  $\alpha+\beta$  and the  $\beta$ -Ti alloys is that there is more  $\alpha$ -phase present in the  $\beta$ -Ti alloys after low temperature aging, and there are consequently far more  $\alpha$ - $\beta$  interfaces available as slip barriers. A second important difference concerns  $\alpha$ -phase nucleation. In the  $\alpha+\beta$  alloys,  $\alpha$ -phase is either formed by a Widmanstatten type of transformation, or by the tempering of martensite. The former often leads to a colony microstructure, of the sort which has never been developed in a  $\beta$ -Ti alloy. Moreover,  $\alpha$ -phase nucleation tends to be substantially more sluggish in the  $\beta$ -Ti alloys. Although this has distinct advantages with regard to hardenability, it makes it difficult to achieve a uniform  $\alpha$ -phase distribution. It is therefore very important to identify and control the mode of  $\alpha$ -phase nucleation in  $\beta$ -Ti alloys. There are five basic types of nucleation sites for  $\alpha$ -phase precipitation: on extant  $\omega$ -phase particles, on  $\alpha''$  plates,  $\alpha$  plates (sympathetic nucleation), on dislocations, and on grain boundaries. The first three involve the presence of some other phase, the last two do not. Each of these types of sites will be discussed below.

At low temperatures (300-500°C)  $\alpha$ -phase nucleation is preceded by the  $\omega$ -phase formation and is strongly influenced by the extant  $\omega$ -phase particles. This influence appears to be stronger in high misfit, cuboidal  $\omega$ -phase forming systems than in low misfit, or ellipsoidal systems (53,64); there is little doubt, however, that  $\omega$ -phase can enhance  $\alpha$ -phase nucleation even in low misfit systems (e.g., TiMo (65)). The exact nature of these nucleation processes remains largely unknown due to artifacts associated with thin-foil relaxation effects and the difficulty in resolving dislocation structures in the  $\beta$ -phase. Nevertheless, convincing micrographs (such as that shown in Fig. 10) seem to indicate that at least in the high misfit systems, the  $\omega$ -phase particles first lose coherency, and then  $\alpha$ -phase nucleates on the interface ledges that are produced (66). Alpha formed in such a fashion is extremely fine, uniform, and tends to adopt a stubby plate morphology (Fig. 11). In the early stages of the  $\omega \rightarrow \alpha$  transition, this variety of  $\alpha$ -phase can only be resolved by TEM; it is optically visible only through artifacts of etching - an accelerated darkening of what appears to be uninterrupted  $\beta$  matrix. During later stages of aging, the  $\alpha$ -phase grows, but seems to maintain its "stubby" morphology. One should note that this nucleation influence is observed in all commercial alloy compositions: Transage 134 (29), Ti-10-2-3 (10), Ti-15Mo-5Zr-3Al (67), and Beta-III (53). In addition, there has been at least one report of direct  $\omega \rightarrow \alpha$  transformation in a composition which would have to be considered "rich": TC6 (Ti-4Al-7Mo-10V-3Cr) (68). This seemingly spurious result may simply be a result of the high oxygen content of the alloy. The  $\omega$  and  $\alpha$  phases have been observed together, in a state of co-existence, in several of the alloys (most notably in Beta III) (53). Apparently,  $\alpha$ -phase forms in an almost compositionally invariant way, having no long range effects upon the surrounding  $\beta$ -phase matrix (16). Thus, the appearance of  $\alpha$ -phase in a microstructure does not immediately destabilize the surrounding  $\omega$ -phase dispersion, but instead the two phases co-exist for some period of time.

(\*The crystallographic nature of non-Burger's  $\alpha$  is complex and is not a phenomenon peculiar to the  $\beta$  alloys. It will therefore not be discussed in this review. The subject has been extensively reviewed by other researchers (26,61,62); there is even some evidence that it may be an artifact, and not present in bulk materials (63).

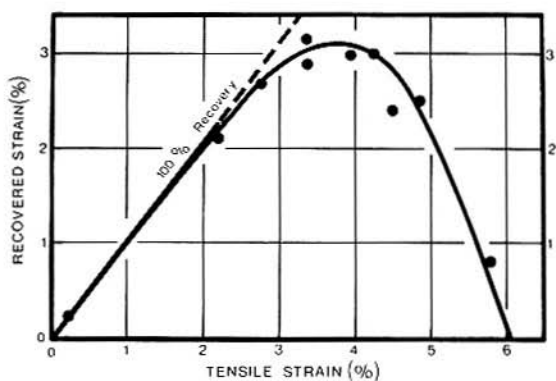


Figure 9. Shape memory recovery as a function of original deformation; the dashed line illustrates perfect shape memory recoveries.



Figure 10. Ledges forming upon cuboidal  $\omega$  in a Ti-V alloy during final stages of  $\omega$ -phase stability.

Due to the extremely fine size and uniform distribution of  $\alpha$ -phase nucleated in the above manner, it is an extremely effective way of strengthening the  $\beta$  matrix. Unfortunately, the resulting dispersions are so fine, and strengths so high, that there is little or no plastic ductility in the peak aged condition. The properties very closely resemble those of  $\beta+\omega$  dispersions. Although ductility can be increased somewhat by resorting to a very low temperature solution treatment, the primary  $\alpha$  volume fractions that result become extremely high. The large strength differential between the soft  $\alpha$  and the rigid matrix leads to mismatched deformation characteristics and premature fracture - a point which will be taken up in more detail later. In any case, decreasing alloy strength by adding large volume fractions of a soft phase does not properly solve the ductility problem; to do that, one must severely overage the  $\beta$  matrix so that its deformation characteristics more closely resemble those of the primary  $\alpha$ . Due to the low temperatures at which  $\omega$ -phase influences  $\alpha$  precipitation, and due to the slow overaging characteristics of the  $\beta$ -Ti alloys, controlling strength via overaging is an impractical solution, requiring several days at temperature even in the best cases. This appears to be more true in the leaner alloys (10) than in Beta-III (53), as would be expected since this sort of nucleation is found at higher temperatures in the more stable alloys. One solution to the problem is to introduce non-isothermal aging techniques: either a two-step (low-high) aging process, or by very slowly heating the material to a higher aging temperature. In both cases, the time spent at the lower temperatures must be long enough to begin the  $\omega\rightarrow\alpha$  reversion process so that the time at the high temperature then controls the growth and coarsening of the  $\alpha$  nuclei. Such techniques have been extensively experimented with on a research basis (10,65), but relatively little has been done to examine their effects upon fracture toughness and to extend the results to large scales. The fracture toughness issue is particularly relevant since the overaged platelets are of a more equiaxed morphology; which usually leads to slightly inferior fracture toughnesses. Still another way to utilize the  $\omega\rightarrow\alpha$  transformation has been proposed and demonstrated in Ti-45%Nb (69). The approach was to again use a duplex aging treatment, but with the high aging temperature first. This has two effects: It reduces the amount of fine  $\omega$  and  $\alpha$  phases that can form during the low temperature aging, but more importantly, the coarse  $\alpha$ -phase plates from the first aging step partition the  $\beta$  matrix, reduce and homogenize slip length, and enhance ductility.

Although we have discussed various ways to encourage  $\alpha$  nucleation by exploiting the  $\omega\rightarrow\alpha$  transition, it is also interesting to consider how  $\omega$ -phase formation can be suppressed. We have already said that direct aging - quenching directly to the aging temperature from the solution treatment temperature-suppressed formation of isothermal  $\omega$ -phase. It should, and in fact does, suppress the occurrence of fine  $\alpha$  (55). A second way to suppress this sort of precipitation sequence is to provide alternate nucleation sites by appropriate thermomechanical treatment or cold work (70).

Another type of nucleation scheme is that of  $\alpha$  upon  $\alpha''$ . There are many ways in which Ti martensites can temper: via the precipitation of discrete  $\alpha$ -phase particles (71), via spinodal decomposition (72), via a reshearing process to  $\beta$  (23,26), and via a direct replacement of  $\alpha''$  with  $\alpha$  via a diffusional process (26,73). In the  $\beta$ -Ti alloys, which are the richest alloys in which martensite can be found, the process would seem to be a combination of the last two, reshearing to  $\beta$ , and the diffusional stabilization of the martensitic plate structure. The diffusional mechanism seems to be the most important in alloys with relatively high  $A_s$  temperatures and with slow heating rates; in alloys with relatively low  $A_s$  temperatures, the reshearing process seems to be more important.

Alpha precipitation via this mechanism does have an important effect upon the tensile strength of the material. In Figure 12, hardenability curves are shown for two lean  $\beta$ -Ti alloys. Tensile specimens were cooled from above the  $\beta$ -transus temperature at various rates, aged, and tested. Of particular interest are the very fast cooling rates, at which both materials were verified to form martensite due to the residual quenching stresses discussed earlier. Hardening was more effective in the water quenched specimens than in the oil cooled specimens where no martensite was found directly after quenching. One implication of this is that one should pay very close attention to residual quenching stresses and the effect they may have upon the final tensile properties of the material. One final comment concerning  $\alpha$ -phase nucleation upon martensite concerns the proposals of Crossley regarding isothermal martensite in the Transage alloys (35,36). Crossley has stated that the hardening during isothermal aging of the Transage alloys is brought about by the compositionally invariant growth of the "sub microscopic" martensite. It is said that growth occurs during aging because of the continuous annealing and recovery of accommodation defects in surrounding the martensite plates. Other studies have demonstrated that structural changes do, in fact, occur while isothermally aging Transage (37), and that the lattice parameters (i.e., the compositions) of the  $\beta$  and  $\alpha$  phases are changed. This would seem to indicate that hardening is brought about by the precipitation of  $\alpha$ -phase, not by an isothermal martensite mechanism. Mechanical twins have also been shown to influence precipitation at high aging temperatures (53), though one would expect the effect to be less pronounced than that due to  $\alpha''$  since the surface energy of a twin interface is comparably quite low.

The third nucleation scenario involves an extant phase in the local enhancement of  $\alpha$  nucleation due to the proximity of extant  $\alpha$  plates - an event which has been termed "sympathetic" nucleation (74). Once one  $\alpha$ -phase plate is nucleated, either on a dislocation, a grain boundary, or as a random event, the incidence of  $\alpha$ -phase nucleation in the immediate surroundings of the first plate is greatly enhanced. This nucleation scheme is generally active in materials which have not martensitically transformed, and at higher temperatures than the  $\omega \rightarrow \alpha$  sequence described earlier (10,27). The microstructural result of this nucleation scenario is to develop clusters of  $\alpha$ -phase plates (Fig. 13(a)). This is most notable in underaged materials, in which these clusters can be observed in a primarily untransformed  $\beta$  matrix; during later stages of aging, or during aging at higher temperatures, the clusters grow together and take on a quite uniform appearance. This variety of  $\alpha$  is always substantially coarser than the  $\alpha$  produced by the  $\omega \rightarrow \alpha$  sequence, and tends to be much more acicular (Fig. 13(b)). One obvious advantage of such a microstructure is that one is not left with the extremely strong and brittle  $\alpha + \beta$  mixture that results from the  $\omega \rightarrow \alpha$  sequence, and non-isothermal aging techniques need not be used.

In addition to nucleation upon extant phases, nucleation is clearly affected by defects; primarily dislocations and grain boundaries. It is well-known that cold working prior to aging accelerates the hardening process and increases the maximum hardness value (53). Unfortunately, it is difficult to say how much of this increase is due to the  $\beta \rightarrow \alpha'' \rightarrow \alpha$  transformation, and how much is due to nucleation enhancement by irreversible slip. With the exception of Beta III, the lean  $\beta$  alloys are generally not cold worked prior to aging; in hot worked or annealed materials, there are too few dislocations in the matrix for this mechanism to be of real direct importance. In these materials, the primary importance of the dislocations is very likely as initiators of the sympathetic nucleation process. There can also be complications to the simple approach that cold work increases strength: it is also well-known that cold work suppresses  $\omega$ -phase formation in favor of direct nucleation of the  $\alpha$ -phase (53), which could, in some cases, supersede the  $\omega \rightarrow \alpha$  mechanism discussed above, lead to coarser  $\alpha$ -phase distributions, and lower



Figure 11. Typical fine, stubby  $\alpha$ -phase that results from nucleation in an  $\omega$ -phase dispersion. (Ti-10-2-3  $\beta$ -solution treated and aged 1 h at 500°C).

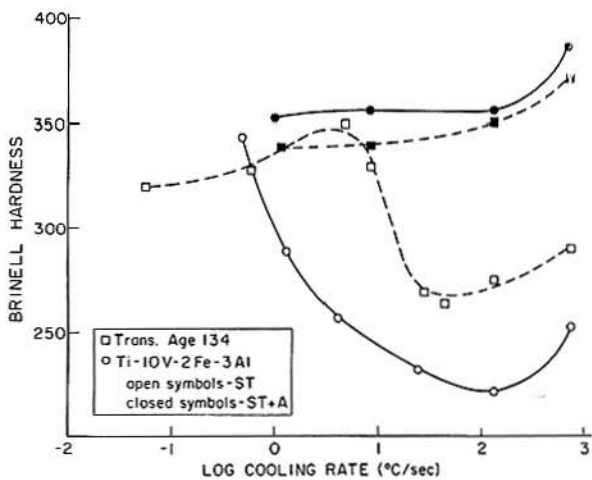


Figure 12. Hardnesses of two lean  $\beta$  alloys (Transage 134 depicted by squares and Ti-10V-2Fe-3Al by circles) after solution treating above the  $\beta$ -transus temperature, cooling at various rates; shown both in the as-cooled condition (open symbols) and after aging (filled symbols).

strengths.

Another type of nucleation site that becomes increasingly operative at the higher temperatures are grain boundaries and sub-grain boundaries. At high temperatures, a continuous layer of  $\alpha$ -phase can be found along the grain boundaries of recrystallized material (Fig. 14); at lower temperatures, and in non-recrystallized material, the layer becomes discontinuous, and often invisible to optical microscopists, but it seems to be very difficult to completely eliminate. Exactly how much harm is done by the presence of such a soft continuous layer is not completely clear, though there is little doubt that it is detrimental to strength, ductility, and toughness (10,75,76). Grain boundary  $\alpha$  becomes even more prevalent in richer alloys and its effect on properties will be discussed in a later section of this article.

**2.1.6 Intermetallics, Inclusions, and  $\beta$  Flecks.** Most of the commercial lean  $\beta$ -Ti alloys do not intentionally contain large amounts of eutectoid-type alloying additions (i.e., Fe, Cr, Mn, and Ni). The reason for this is that these create the possibility of intermetallic compound formation during high temperature service exposures, leading to degradation of mechanical properties (77). Nevertheless, all commercial  $\beta$ -Ti alloys do contain inclusions; a greater amount than would typically be found in  $\alpha$  and  $\alpha+\beta$  alloys. These inclusions do not generally affect strength (with the possible exception of the inclusions found in Transage which are claimed to be  $ZrFe_2$  (78)). Moreover, the effect of these inclusions on void formation and ductile fracture appears to be significant only in the unaged conditions (10). There is, however, evidence that the inclusions affect grain growth, and in this respect can have an indirect effect on mechanical properties (Fig. 15).

A second type of microstructural defect, and one of apparently greater significance, is the so-called " $\beta$  flecks".  $\beta$  flecks (see Fig. 16) are simply regions enriched in  $\beta$ -stabilizing elements - usually Fe or Cr. Both Fe and Cr tend to segregate from Ti, and therefore tend to form regions which have a lower  $\beta$ -transus (or greater  $\beta$ -phase stability) than the surrounding composition. Even though the local chemical variations can be quite small, their effect upon microstructures can be quite dramatic in material solution treated just below the  $\beta$ -transus temperature of the bulk material. Alloy compositions which do not contain  $\beta$  eutectoid additions such as Fe, Cr, and other powerful  $\beta$ -stabilizing additions tend not to suffer as much from this problem, but unfortunately, Fe and Cr additions are more effective solid solution strengtheners of the  $\beta$ -phase than the isomorphous  $\beta$ -stabilizers, Nb, Mo and V.

## 2.2 Mechanical Properties:

Several general comments pertaining to the strength of the lean  $\beta$ -Ti alloys have already been incorporated into the microstructural discussion. To summarize, it has been mentioned that the strength of the unaged condition is controlled by the onset of a stress-induced martensitic transformation and mechanical twinning; the strength of the  $\omega$ -aged conditions are extremely high, owing to the extremely fine nature of the  $\beta+\omega$  dispersions; the strengthening ability of  $\alpha$ -phase precipitates is derived from the high density of  $\alpha$ - $\beta$  boundaries even though the  $\alpha$ -phase particles themselves are quite soft. In addition, a correlation between solution treatment temperature, attendant  $\beta$  stability, and aged strength was demonstrated in Figure 3: higher solution treatment temperatures generally lead to higher strengths. One exception to this rule appears to exist whenever a decrease in solution treatment temperature prevents recrystallization; in this case, the enhancement of  $\alpha$ -phase nucleation can outweigh considerations of  $\beta$ -matrix stability and an increase in strength with decreasing temperature can be observed. Some overaging trends were also presented: it was said that the  $\beta$ -Ti alloys tend to have very

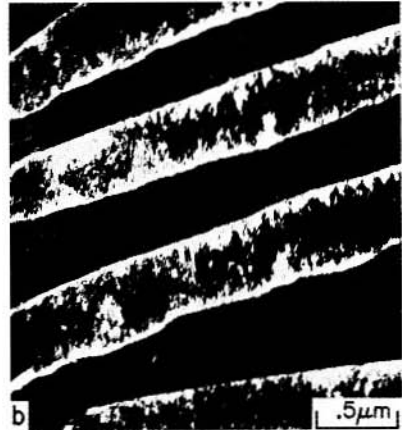
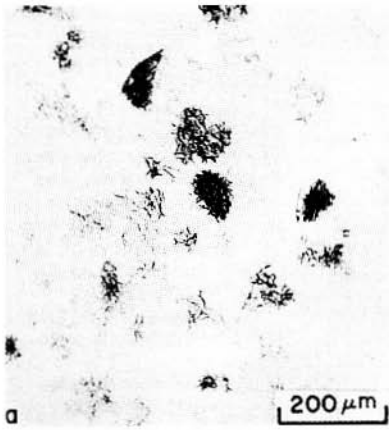


Figure 13. Sympathetically nucleated  $\alpha$  in Ti-10-2-3  $\beta$ -solution treated and aged at 600°C. a) light micrograph, b) TEM micrograph.

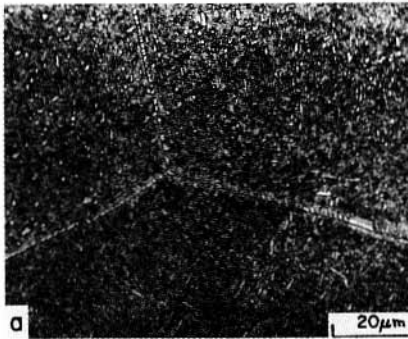


Figure 14. Preferred precipitation of  $\alpha$  on grain boundaries (a), and upon sub-boundaries (b).

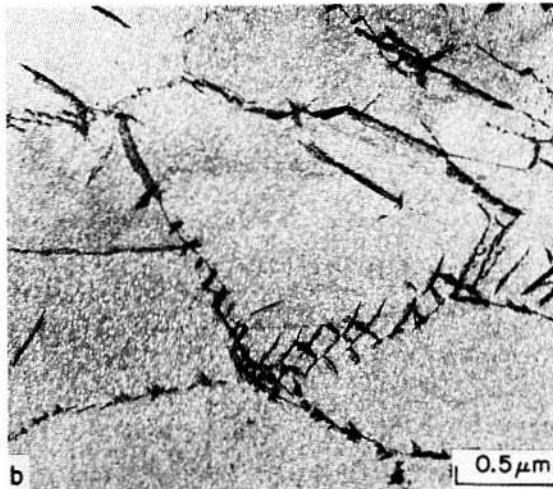






Figure 15. TEM micrograph showing an example of how inclusions can pin  $\beta$  grain boundaries.

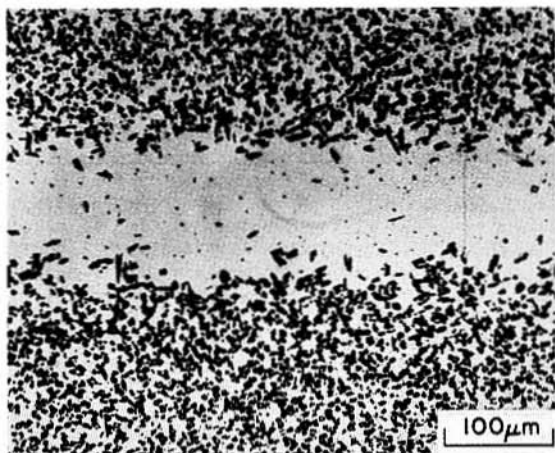


Figure 16. Illustration of chemical segregation due to local iron enrichment.



asymmetric aging behaviors, with rather rapid hardening during the early stages, and very sluggish overaging. Finally, the importance of controlling  $\alpha$ -phase nucleation was discussed: the importance of the aging temperature, of the rate at which the specimen is brought to that temperature, of cold work, and of two-step aging treatments.

One can see that the strength of these alloys can be manipulated in a variety of ways. For example, an increase in strength can be affected by reducing primary  $\alpha$  content (raising solution treatment temperature), reducing the aging temperature, altering the aging time so that strength is closer to its peak value, by resorting to a duplex aging treatment (or by slowly heating to the aging temperature), by introducing martensite before aging, and by altering the TMP to provide a higher defect concentration after solution treatment. Thus, the question to address next, is: "Given an application with a certain strength requirement, what is the optimum way to achieve that strength?" This depends, of course, on what other properties are critical. We have already mentioned, for example, that one might choose a  $\beta$ -processed alloy in toughness critical applications, and might prefer an  $\alpha+\beta$ -processed material in applications that are ductility critical. With so many different routes to take to a final microstructure and set of properties, it is impossible to be specific about properties and microstructures. Certain trends in the properties are, however, evident and can be separately discussed.

2.2.1 Ultimate Tensile Strength. Given a certain yield strength level, it is possible to have quite different UTS values. For example, in Ti-10-2-3 strengthened to a yield strength of 1225 MPa, one can achieve UTS values ranging from 1260 to 1420 MPa (14). Mechanically, this is due to the stability of necking, or the strain hardening rate. As one might expect of a microstructure strengthened by shearable particles,  $\omega$ -phase strengthening also leads to the lowest work hardening rates and the lowest UTS values (on a yield strength normalized basis). Within the  $\alpha$ -aged microstructures, coarser distributions of fine  $\alpha$  tend to have the lowest work hardening rates and lowest UTS values. Of course, if one is to achieve the same yield strength in the two conditions (coarse and fine  $\alpha$ ) one must manipulate the solution treatment temperature. This is demonstrated below.

Table I. Properties of Two Heat Treatment Conditions of Ti-10V-2Fe-3Al

<u>Heat Treatment</u>	<u>YS</u> <u>(MPa)</u>	<u>UTS</u> <u>(MPa)</u>	<u>Elongation</u> <u>(%)</u>
1 hr at 800°C then 4 hrs at 500°C	1225	1318	8.7
4 hrs at 720°C then 15 hrs at 370°C	1225	1405	9.5

In the case of the  $\omega$ -aged condition, the low work hardening rate is consistent with the proposition that the particles are being sheared and resistance to dislocation passage significantly reduced upon yielding (79,80). The case of the  $\alpha$ -aged conditions is less clear, but one must surmise that the finer distribution of dislocation barriers ( $\alpha$ - $\beta$  interfaces) promotes dislocation tangling, and more rapid work hardening.

Ductility:  $\beta$ -Ti alloys in general tend to exhibit greater scatter in ductility than do the  $\alpha$  and  $\alpha+\beta$  alloys. This scatter can be found both between ingots and within the same ingot, and would seem to be primarily due to

$\beta$  flecks (11,81). Other microstructural inhomogeneities such as grain boundary  $\alpha$  may also be a contributing factor. Although there has recently been progress towards the elimination of these problems, one should be aware that ductility data from one source may not necessarily agree with that of another source. Although this makes it somewhat difficult to study ductility systematically, many microstructural trends have been identified. Several of these are illustrated in Figure 17:

1. There is, as in most alloys, a general decrease in ductility as the strength of the alloy is increased. Moreover, the slope of ductility loss is not constant, but instead depends strongly upon microstructure.

2. Given any specific strength level, the most brittle microstructures are the  $\beta$ -solution treated and aged microstructures.

3. The most ductile microstructures are those solution treated very close to, but not above, the  $\beta$ -transus temperature. Recalling earlier discussions, these microstructures are the finest grain microstructures; they have been allowed to recrystallize during solution treatment, but the small volume fraction of primary  $\alpha$  has prohibited grain growth.

4. Increasing the amount of primary  $\alpha$  beyond the minimum which is necessary to inhibit grain growth decreases ductility.

5.  $\omega$ -aged microstructures, although generally quite brittle, can be made more ductile by refining grain size.

Many of the aforementioned observations can be rationalized on the basis of slip homogeneity (76), and with the understanding that fracture is caused by a void coalescence mechanism. To discuss this, it is necessary to first summarize some of the basic deformation features of these alloys. Voids form at  $\alpha$ - $\beta$  interfaces in aged microstructures, at slip band intersections in  $\omega$ -aged microstructures, and at inclusions in unaged microstructures (76). As already mentioned, the  $\alpha$ - $\beta$  interfaces behave as partial slip barriers; there are a sufficient number of common slip systems transferred between the  $\alpha$  and  $\beta$ -phases through the Burger's relationship so that slip can pass through the barrier once there is a sufficient concentration of slip behind the barrier (82,83). In addition, the resistance of these  $\alpha$ - $\beta$  interfaces to penetration appears to be dependent upon the particle size distribution; distributions of smaller particles tend to be more resistant to passage than are distributions of larger particles (84). This may be because of the greater concentration of transformational defects in the  $\beta$ -matrix (83), or because it is more difficult to obtain the critical stress concentration when the slip lengths are small. Typical  $\beta$ -Ti alloy microstructures are bimodal; they consist of a strong  $\alpha$ + $\beta$  matrix, with soft monolithic  $\alpha$  at the grain boundaries and distributed throughout in the form of primary  $\alpha$ . Increasing the strength difference between the soft  $\alpha$ -phase and the harder  $\alpha$ + $\beta$  mixture in the matrix encourages localized deformation, and low apparent deformations. Finally, it has been proposed that only grain boundaries are able to reduce slip length in these alloys; one might think sub-grain boundaries and primary  $\alpha$  particles would be effective slip barriers, but this seems not to be the case (76).

The first of the above observations (decreasing ductility with aging) is simply rationalized on the basis that aging increases the frequency of  $\alpha$ - $\beta$  interfaces, which increases the frequency of void formation. The second of the above observations, that  $\beta$ -solution treated microstructures are the most brittle, is explained by the fact that the grain boundary  $\alpha$  layer is most pronounced in this condition, and deformation is being concentrated in these soft regions; thus, the microscopic strains are extremely high, even though the

macroscopic strains are relatively low. The third observation is best understood on the basis that finer grain sizes tend to reduce slip length, intensity and nonhomogeneity. The decrease in ductility as the volume fraction of primary  $\alpha$  is increased (the fourth observation) occurs because the strength differential between the soft primary  $\alpha$  and the rigid  $\beta$ -matrix is increasing. Increasing this strength differential delays the onset of matrix deformation, concentrates the more strain in the primary  $\alpha$ , and leads to a premature failure. The last observation, relating to the  $\omega$ -phase, has already been discussed to some extent. Decreasing the  $\beta$  grain size of  $\beta+\omega$  microstructures homogenizes slip by reducing slip length, and therefore delays crack nucleation. In large grained materials, as little as a 0.6% volume fraction of  $\omega$  is thought to be completely embrittling (59).

There is one more microstructural factor which affects ductility but which is not demonstrated by Figure 17. This is the role of primary  $\alpha$  morphology. It has been well documented that higher TMP temperatures lead to more acicular primary  $\alpha$  morphologies and reduced ductility (75,11,85). This, in conjunction with the need to eliminate grain boundary  $\alpha$ , is why the lean  $\beta$ -Ti alloys are normally finish forged, or rolled, in the  $\alpha+\beta$  phase field. The reason for this ductility decrease is not entirely clear, although it has been proposed that it is due to the high density of voids which nucleate on the plane of the  $\alpha$  plates at the  $\alpha$ - $\beta$  interface (75,86).

There is a strong directionality to ductility: ductilities measured parallel to the working direction tend to be higher than those perpendicular to the working direction. This result is not easily explained on the basis of texture, since the [1 1 0] directions are known to have the highest work hardening rates and best ductilities, but it is the [1 1 1] directions which are preferentially aligned in the working direction. To some extent, the directionality can be rationalized on the basis of primary  $\alpha$  shape; in heavily worked microstructures, the primary  $\alpha$  is elongated parallel to the working direction. The most rapid void formation would be expected to occur when the major axis is oriented perpendicular to the tensile axis. This would be most harmful to the transverse ductility. Although this may be part of the story, it fails to explain ductility anisotropy in  $\beta$  solution treated and aged materials (i.e., with no primary  $\alpha$  present). Thus, the directionality of tensile ductility in  $\beta$ -Ti alloys is not well understood.

**2.2.2 Elastic Modulus.** The moduli of the  $\beta$ -Ti alloys tends to be lower than those of the  $\alpha$  and  $\alpha+\beta$  alloys. For structural applications, this is more often than not a detriment. There are spring related applications, however, which require a material capable of storing large amounts of elastic energy(\*) In these terms, the  $\beta$ -Ti alloys excel. The  $\beta$ -Ti alloys are capable of storing upwards of 4.5 Newton-meter/gram - over twice the capability of steel. Even so, spring applications for  $\beta$ -Ti alloys are not particularly common, and the alloys which are commercially best known have compositions designed to maximize modulus, not to maximize elasticity. There clearly are a variety of compositional changes that could be made to improve the suitability of these alloys for spring applications - decrease aluminum content, for example - but even within the bounds of fixed and "known" compositions, one observes a microstructural dependence of modulus (unlike most metals). The  $\beta$ -phase possesses a notably lower modulus than that of the  $\alpha$  or  $\omega$ -phases, on the order of 16% lower than  $\alpha$  and 50% lower than  $\omega$  (87). One therefore finds that unaged microstructures have lower moduli than aged structures. One would also expect, though it has never been systematically proven, that underaged microstructures should have lower moduli than overaged microstructures.

(\*) The stored elastic energy per gram of load bearing member is  $\frac{\sigma^2}{E \cdot \rho}$  where  $\sigma$  is the stress, E is Young's modulus and  $\rho$  is the density.

2.2.3 Fracture Toughness. Controlling the fracture toughness of lean  $\beta$ -Ti alloys in the aged condition has been an important issue to the aircraft industry for several years (11,13,35,75,88,89). All of these studies report findings which do not always parallel those reported in the  $\alpha+\beta$  alloys (90-92). For example, increasing the processing and solution treatment temperatures can increase or decrease toughness, depending on strength level. One should note, however, that ductility shows a more consistent trend; higher processing or solution treatment temperatures usually lead to higher strengths and reduced tensile ductility. After fixing the strength level of an alloy, the ductility or toughness can be varied and improved, but it is generally not possible to simultaneously improve both. Therefore, one must try to achieve a desirable compromise. There is a similar trade-off in the solution treatment temperature, but not as obvious. The most fracture resistant microstructures are usually the least ductile ones ( $\beta$ -solution treated), but one can achieve an interesting blend of properties by solution treating some 10-30°C below the  $\beta$ -transus (93).

The above microstructural influences have been suggested to be related to crack "tortuosity" (94) - that is, the extent to which a crack is deviated from its most direct route, and the extent to which a microstructural condition promotes secondary cracking. Tortuosity, then, is a qualitative way of describing how much energy a material absorbs through frequent, microscopic deviations of the crack path and by forcing the crack to follow multiple paths. Considering the conventional wisdom that crack growth preferentially follows  $\alpha$ - $\beta$  interfaces, (for which there is ample evidence), one can then suppose that highly elongated or acicular  $\alpha$  would tend to deviate the crack path to the greatest extent, lead to the greatest tortuosities, and to the best toughnesses. These arguments qualitatively agree with the observed toughness trends inasmuch as increasing the TMP temperature tends to produce more acicular primary  $\alpha$ . Increasing the solution treatment temperature also implies that aging will be done at higher temperatures and therefore obtain more elongated fine  $\alpha$  will be formed. In the  $\alpha$  and  $\alpha+\beta$  alloys, it is the colony type of microstructures which are generally the most fracture resistant. Unfortunately, it does not seem possible to generate similar  $\alpha$  alignments in the  $\beta$ -Ti alloys, probably because the lower transformation temperatures limit the size of the diffusion fields which control  $\alpha$ -plate size. There also is a microstructure scale effect which pertains to toughness/microstructure variations. If the  $\alpha$ -plates are small compared to the crack tip plastic zone size at the onset of crack extension, then plate size and shape are not effective in deflecting the crack and microstructure becomes less important. Since the plastic zone size scales with the inverse square of the yield stress, this often leads to microstructurally insensitive toughnesses in  $\beta$ -Ti alloys.

The effects of other microstructural features also are noteworthy. The fracture toughnesses of  $\omega$ -aged structures, as one might expect, is quite low compared to  $\alpha$ -aged structures (53,95). This is due to the extreme localization of slip and the rapid extension of cracks. It has also been established (89,96,98) that grain boundary  $\alpha$  is detrimental to toughness. Grain boundary  $\alpha$  encourages the crack to follow an intergranular route, and even though the route is macroscopically more tortuous than a transgranular route, the path itself is entirely along  $\alpha$ - $\beta$  interfaces, and therefore a low energy path (85,97,98). One more microstructural feature which has been mentioned in connection with increasing toughness is the stress-induced transformations at a crack tip can increase the fracture toughness of the Hadfield and TRIP steels (99), as well as certain ceramics (100); some limited work with 10-2-3 suggests that the same trend is followed (101). Crossley (35,102) has said that the stress-induced martensitic transformation has an important effect upon the toughness of fully aged Transage alloys. It seems doubtful, however,

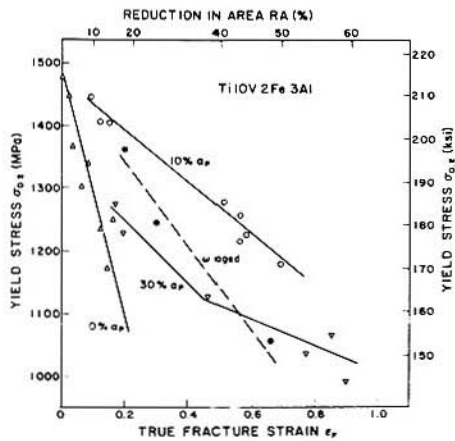


Figure 17. Demonstration of how the ductility of Ti-10-2-3 decreases with increasing strengths in various microstructural conditions.

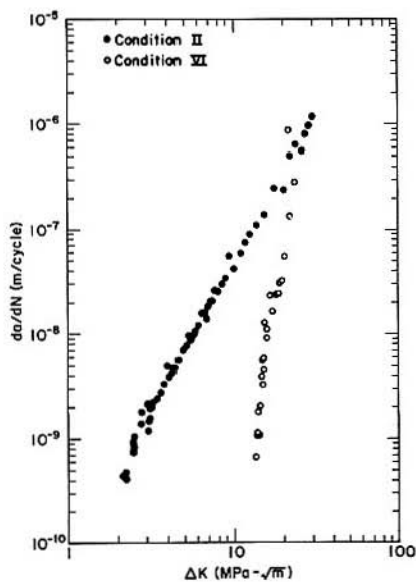


Figure 18. Comparison of  $da/dN$  in  $\alpha$ -aged (closed circles) and  $\omega$ -aged (open circles) conditions of Ti-10-2-3 aged to equal yield strength levels.

that one could still obtain a martensitic transformation in a lean  $\beta$ -Ti alloy composition after aging to, or beyond, peak hardness. Moreover, there is enough evidence that underaged microstructures have poorer toughnesses than overaged to look elsewhere for explanations of the purported high toughness of Transage.

2.2.4 Fatigue. Our discussion of fatigue will be divided into two parts. First, fatigue crack growth will be discussed, then a summary of fatigue crack initiation and smooth bar fatigue life will follow.

Systematic studies of fatigue crack growth rates in the  $\beta$ -Ti alloys have been rather limited. Chakraborty, et al have measured growth rates of several rather rich Ti-V alloys, and demonstrated a tendency toward increased crack growth rates as slip becomes more homogeneous (103,104). In terms of the commercial  $\beta$ -Ti alloys, only two systematic attempts have been made to relate microstructure to Fatigue Crack Growth (FCG): Ti-10V-2Fe-3Al (14,97) and Beta-III (95). Both studies showed that FCG is significantly slower in  $\omega$ -aged microstructures than in  $\alpha$ -aged microstructures of equal strength (Fig. 18). In Ti-10-2-3, the threshold cyclic stress intensity was increased from  $\sim 2 \text{ MPa}\cdot\text{m}^{1/2}$  to  $\sim 9 \text{ MPa}\cdot\text{m}^{1/2}$ . Unlike other alloys where such effects have been seen, this rather large increase could not be attributed to changes in modulus (105), since  $\omega$ -phase precipitation increases modulus and should therefore increase FCG, all else being equal. The improvement was instead attributed to changes in slip reversibility. The central idea here is that microstructures which exhibit coarse, planar slip will not allow the accumulation of damage in a plastic zone as quickly as microstructures which undergo homogeneous, or wavy slip (106). This argument has been used to explain FCG rates in Ti-Al alloys (107,108), as well as the Ti-V alloys mentioned above (103,104).

In contrast, these studies showed that FCG was invariant to microstructural changes in  $\alpha$ -aged microstructures of equal strength (Fig. 19). In Ti-10-2-3, for example, 10 distinct microstructural conditions were tested, the microstructures included changes in grain size, extent of recrystallization, nature of fine  $\alpha$ , and the primary  $\alpha$  shape, size and volume fraction. All conditions proved to exhibit very similar crack growth characteristics in the threshold and Paris Law growth regimes. At the very fast FCG rates, there were small differences, and the materials could be ranked in order of their anticipated fracture toughness values (see previous section). One would conclude, then, that slip inhomogeneity and reversibility were not affected by these changes.

In a separate study (101), unaged microstructures of the same material were shown to have significantly reduced FCG rates. It is not clear, however, whether these improvements are due to the disappearance of  $\alpha$ - $\beta$  interfaces, or whether the improvements were brought about by the stress-induced martensitic transformation. Studies of the Beta-III alloy showed similar results when  $\beta$ -solution treated and  $\alpha$ -aged microstructures were compared. Since Beta-III does not transform martensitically, this suggests that there is an intrinsic microstructure effect. Studies in TRIP steels have shown that a martensitically transforming plastic zone leads to significantly reduced growth rates (109). Thus, the effect observed in Ti-10-2-3 may result from a combination of these two factors.

One might be tempted to conclude from the above discussion that  $\omega$ -aged conditions are preferable in fatigue critical applications. The picture presented here, however, is incomplete since we have not yet discussed microstructural influences upon crack initiation. It is often the case that microstructures which show excellent FCG resistance through the above slip



reversibility mechanism also show poor smooth bar fatigue lifetimes (107). Coarse planar slip leads to high reversibility, but also accelerates crack initiation via the intersection of these coarse and intense slip bands with boundaries and with one another. It has been fairly well established that  $\omega$ -aged conditions exhibit poorer smooth bar fatigue lifetimes than do the  $\alpha$ -aged conditions (110), especially in the stress regime where significant local plastic strains are accumulated. Reducing the grain size of  $\omega$ -aged conditions has the beneficial effect of homogenizing slip. Some results indicate that grain size reductions may provide sufficient homogenization to approach fatigue lifetimes of  $\alpha$ -aged conditions (111). This always is accomplished, however, at the expense of slip reversibility, and therefore FCG resistance. Unfortunately, very little work has been done to compare the smooth bar fatigue characteristics of various  $\alpha$ -aged microstructural conditions of equal strength level, and determine what microstructural features are optimum for smooth bar fatigue applications. This is clearly an area where more work is required.

### 3.0 Solute Rich $\beta$ -Alloys

The rich  $\beta$ -Ti alloys differ in several respects from the lean alloys discussed earlier. First, by the definition mentioned earlier, they don't form athermal  $\omega$ -phase. Second, they exhibit a phase separation reaction in which the  $\beta$ -phase decomposes into two b.c.c. phases (Fig. 20), one solute rich and one solute lean; the solute lean phase is designated  $\beta'$ . Third, the  $\alpha$ -phase nucleation kinetics are slower in these solute-rich alloys, which means that longer aging times are required to achieve peak strength (Fig. 21) (112). The reasons for this include the typically lower aging temperatures used for these alloys because of the lower  $\beta$ -transus and the greater amount of diffusion that is required to disperse the higher concentration of  $\beta$ -stabilizing solutes during formation of the  $\alpha$ -phase precipitates. However, the nucleation and growth kinetics of grain boundary  $\alpha$  are considerably less sensitive to alloy composition. This is shown schematically in Figure 22. Here, the time difference between the uniform  $\alpha$  nucleation curve and the grain boundary  $\alpha$  nucleation curve increases with increasing solute concentration. As a result, the tendency to form grain boundary  $\alpha$  is more pronounced in these alloys. The importance of this will become clearer when their properties are discussed.

Because of the increased incidence of grain boundary  $\alpha$ , the processing of the rich  $\beta$ -Ti alloys becomes especially important. Unfortunately, the relatively lower  $\beta$ -transus of these alloys leads to high flow stresses at temperatures corresponding to the  $\alpha+\beta$  region, making it difficult, if not impossible, to  $\alpha+\beta$  process these alloys. As a result, grain boundary  $\alpha$  is essentially omnipresent in all of these alloys. However, because of the low transus temperature it also is relatively easy to process these alloys in a way that leads to a minimum amount of recovery and recrystallization, leaving a high density of substructure to aid the nucleation of  $\alpha$ -phase (cf Fig. 14(b)). The kinetics of recovery and recrystallization are relatively slow at temperatures in the vicinity of the  $\beta$ -transus but are also quite dependent on processing history. As a result, the aging kinetics of alloys processed to contain substructure, tend to be highly variable and processing dependent. This places very real, practical restrictions on the use of TMP for enhancing the aging response of these alloys. A few exceptions should be noted here; for example, in the case of springs and fasteners, a heavily cold-worked structure can be conveniently reproduced and then aged to very high strength levels, levels that would be too high to be useful for fracture-critical members. An example of the effect of working to introduce a high dislocation density on the aged microstructure is shown in Figures 23(a)&(b)(112). These

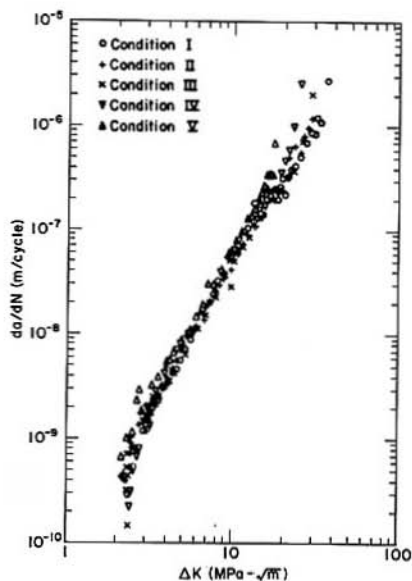


Figure 19. Comparison of  $da/dN$  for various  $\alpha$ -aged microstructural conditions of Ti-10-2-3, showing that microstructure variations of this type have very little effect on FCC rate.

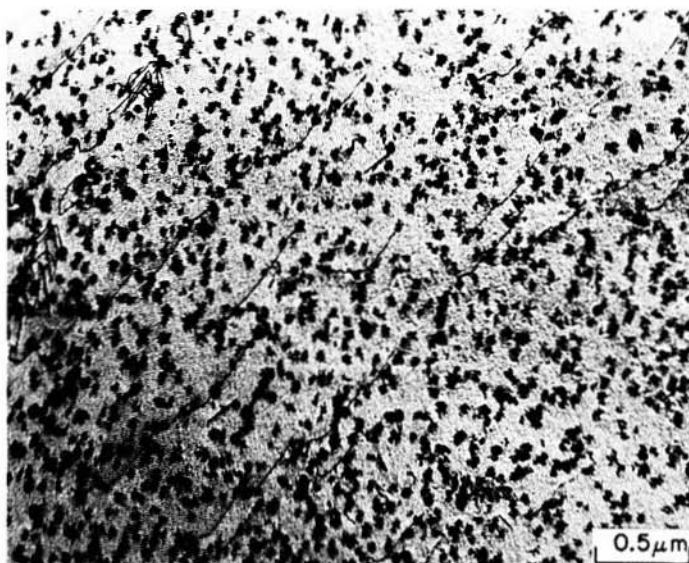


Figure 20. Bright field TEM micrograph showing  $\beta'$  zones in a  $\beta$ -matrix in Ti-8V-8Mo-2Fe-3Al  $\beta$ -solution treated and aged  $250^\circ\text{C}$  for 200 h.



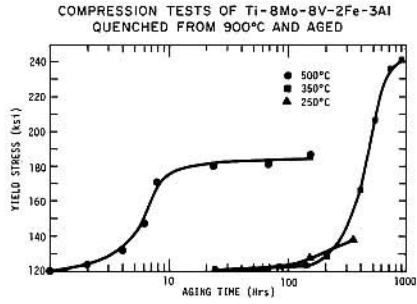


Figure 21. Yield stress vs. aging time curves for Ti-8V-8Mo-2Fe-3Al  $\beta$ -solution treated and aged at 3 different temperatures.

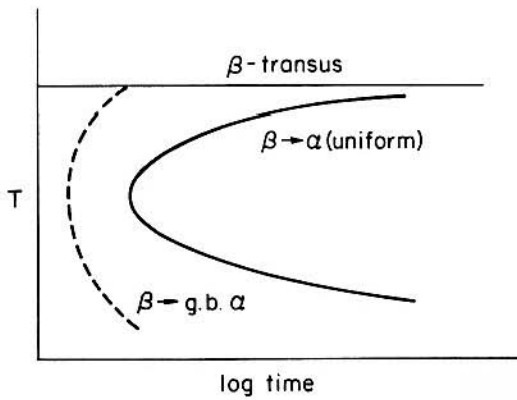


Figure 22. Schematic transformation diagram showing the difference in kinetics of heterogeneously nucleated  $\alpha$  (g.b. $\alpha$ ) and uniformly nucleated  $\alpha$ .

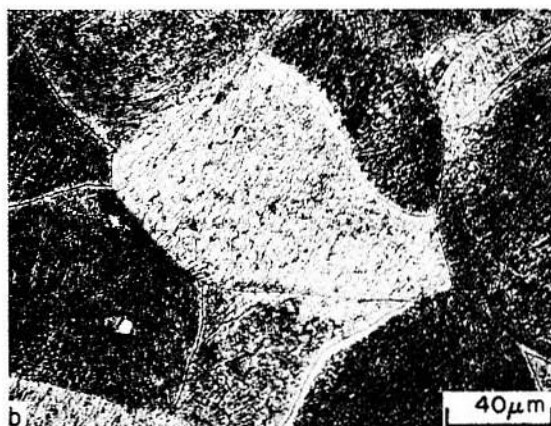
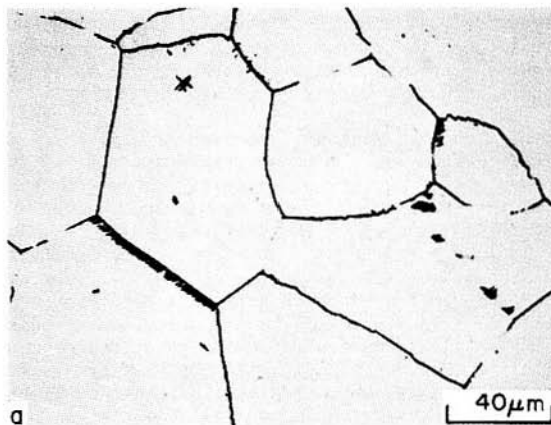


Figure 23. Light micrographs showing the effect of intermediate working on the  $\alpha$ -phase precipitate distribution in Ti-8V-8Mo-2Fe-3Al. a)  $\beta$ -solution treat + aged 1 h at  $650^{\circ}\text{C}$  (no intermediate work), b)  $\beta$ -solution treated, rolled 30% at  $300^{\circ}\text{C}$  + aged 2 h at  $500^{\circ}\text{C}$ .

micrographs also show that the accelerated rate of intragranular  $\alpha$ -phase precipitation also reduces the extent of grain boundary  $\alpha$  formation. The refinement of  $\alpha$ -phase precipitate size and spacing are better seen by TEM. Examples of this are shown in Figures 24(a) and (b) (112).

**Properties of Rich  $\beta$ -Ti Alloys:** The rich  $\beta$ -Ti alloys are normally aged in the temperature regime where  $\alpha$ -phase precipitates directly. In such cases, the aging response obeys the typical sigmoidal-shaped curve, examples of which were shown in Figure 21. One of these is shown again in Fig. 25 (112) in addition to the obvious sigmoidal shape of this curve, it has a shallow, upward slope in the long time regime. This appears to be due to the continued rejection of  $\beta$ -stabilizing solutes into the  $\beta$ -matrix. The evidence for this is the continued contraction of the  $\beta$ -matrix lattice parameter. This is also shown in Figure 25. This additional solute enrichment produces a small additional increment of solid solution hardening which corresponds to the slight positive slope of yield strength-aging time curve. Aging at lower temperatures tends to result in higher strengths, as shown in Figure 21. However, such strengths have low corresponding ductilities, as can be seen in the plots of Figure 26.

Also shown in Figure 26 is the accelerating effect of an intermediate working step on the aging response. From this figure it can be seen that the intermediate worked material reaches peak strength at a shorter aging time than is required to initiate an aging response in the unworked alloy. It is significant to note that the ductilities of both conditions converge to a common value at the same strength level.

From a microstructural viewpoint the aging response can be divided into three temperature regimes: the phase separation regime (lowest aging temperatures), the uniform  $\alpha$ -phase nucleation regime (highest aging temperatures), and the sympathetic  $\alpha$ -phase nucleation regime (intermediate to the previously identified extremes). The microstructures associated with these three are shown in Figures 20, 24(a) and 27. The aging response associated with these three conditions was shown in Figure 21. From this it can be seen that the phase separation reaction has little direct effect on the yield stress. However, a duplex aging treatment consisting of a low temperature age to create the solute-lean  $\beta$ -zones and an intermediate temperature age to precipitate  $\alpha$ -phase on these solute-lean sites, as shown in Figure 28. This can result in high strength levels. Unfortunately, such a heat treatment also results in formation of grain boundary  $\alpha$ . The very fine  $\alpha$ -phase distributions which result from sympathetic nucleation also result in very high strengths but, again, the attendant ductilities are typically low, as shown in Figure 29. Overaging is relatively slow in these microstructures, thus this means of controlling strength has only limited usefulness. The one exception to this is the rapid overaging seen in material which has been given an intermediate working step (Fig. 26). This can be accounted for on the basis of the smaller  $\alpha$ -phase precipitate spacing and the shorter diffusion distances involved in any coarsening reaction. In summary, the rich  $\beta$ -Ti alloys are capable of developing more strength than is generally useful since the ductility values which accompany these strengths are inadequate for most applications.

The reasons for the low ductility of these alloys in the high strength condition is related to the occurrence of intergranular fracture. This fracture mode is the result of grain boundary  $\alpha$  (89,98). At high strengths, the grain boundary  $\alpha$  is much weaker than the matrix. As a result, essentially all of the plastic strain is concentrated in the grain boundary  $\alpha$  which fails by ductile rupture. The fracture surfaces of tensile specimens exhibit predominantly intergranular fracture, but the grain boundary facets contain

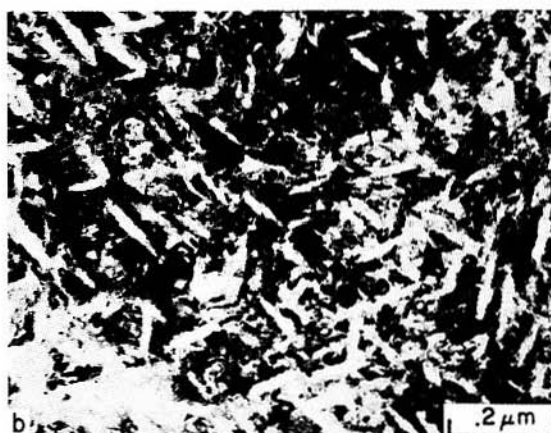
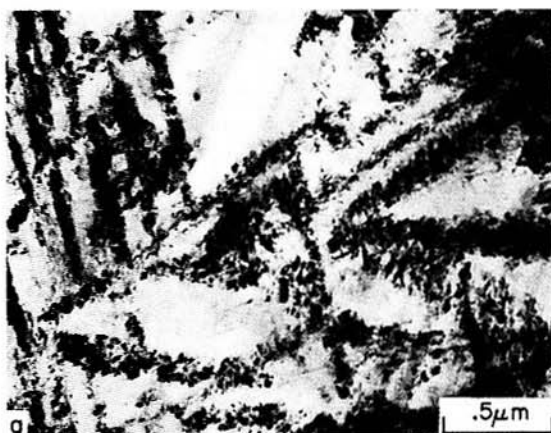


Figure 24. TEM micrographs showing the effects of intermediate working on the  $\alpha$ -phase precipitate size and spacing in Ti-8V-8Mo-2Fe-3Al. a)  $\beta$ -solution treated and aged 2 h at  $500^{\circ}\text{C}$ , b)  $\beta$ -solution treated, rolled 30% at  $300^{\circ}\text{C}$  and aged 2 h at  $500^{\circ}\text{C}$ .

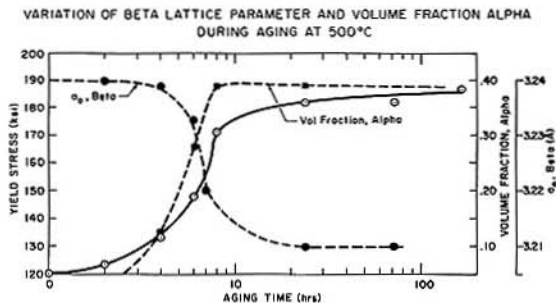


Figure 25. Plots showing the variation in yield strength and  $\beta$ -matrix lattice parameter as a function of aging time for Ti-8V-8Mo-2Fe-3Al aged at 500°C.

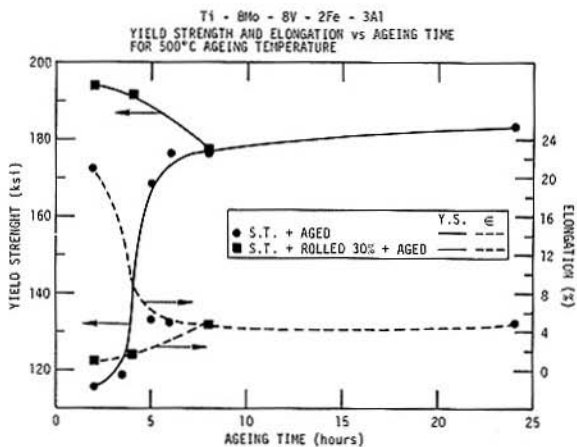


Figure 26. Yield strength and tensile elongation vs. aging time for Ti-8V-8Mo-2Fe-3Al  $\beta$ -solution treated and aged at 500°C with and without an intermediate working step.

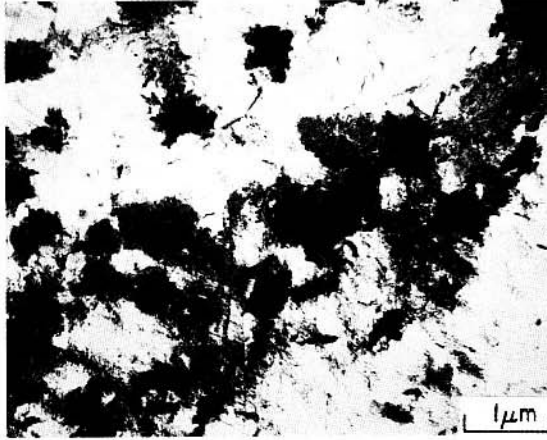


Figure 27. TEM micrograph of Ti-8V-8Mo-2Fe-3Al  $\beta$ -solution treated and aged 385 h at 350°C, showing clusters of  $\alpha$ -precipitates which appear as dark patches.

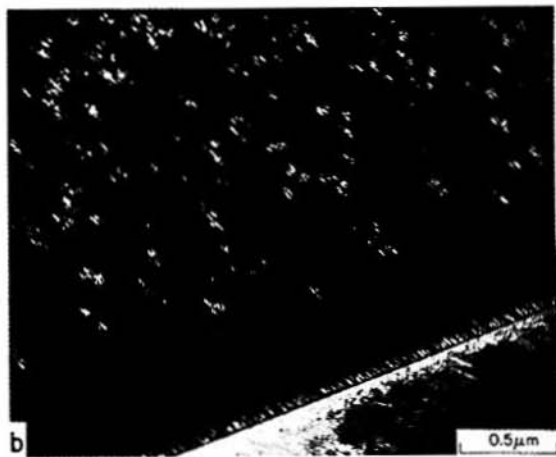
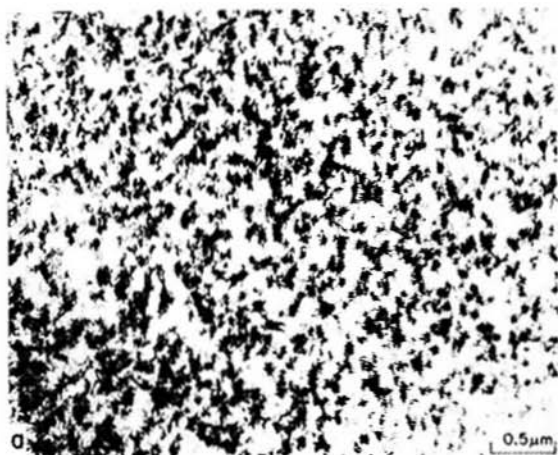


Figure 28. TEM micrographs showing formation of  $\alpha$  on  $\beta'$  and at grain boundaries. a)  $\alpha$  formed on  $\beta'$ , b)  $\alpha$  formed at grain boundaries.

dimples consistent with ductile rupture of the grain boundary  $\alpha$ .

The fracture toughness of rich  $\beta$ -Ti alloys tends to be on the low side also due to the propensity for intergranular fracture. It is possible to alter this fracture mode by  $\alpha+\beta$  processing, but as mentioned earlier, this is generally impractical in this class of alloys. However, the variation in fracture modes that can be produced by processing variations is illustrated in Figure 30. Although there is not a lot of toughness data for commercial rich  $\beta$ -Ti alloy compositions, some representative data for experimental alloys is shown in Table II. These data show that the toughness decreases significantly when the predominant fracture path is intergranular.

The information presented above permits the relationship between microstructure, fracture mode and properties to be generalized as follows. The occurrence of intergranular fracture can increase or decrease toughness, depending on strength level; at low strengths intergranular fracture tends to correspond to higher toughness, whereas at high strengths it does not. A schematic representation of these trends is shown in Fig.31 (113). In contrast, the occurrence of intergranular fracture seems to always correlate with low tensile ductility, as is schematically shown in Figure 32(113). The effect of grain boundary  $\alpha$  on the measured toughness value has been explained by a qualitative model which is summarized in Figure 33 (88). This model is based on the notion that the strength difference between the matrix and the grain boundary  $\alpha$  controls the extent to which the crack tip plastic zone can spread into the matrix. If the strength is large, then the plasticity is confined to the grain boundary  $\alpha$  and the amount of energy dissipated per unit crack extension is small, hence a low toughness value.

The propensity for grain boundary  $\alpha$  formation and the low  $\beta$ -transus temperature combine to make achieving high toughness in these alloys difficult. Studies of experimental alloys have shown (89,98) that  $\alpha+\beta$  processing can significantly improve toughness in the vicinity of the 1200 MPa (175 ksi) strength range. However, reproducible achievement of these strengths in commercial practice may be difficult to realize.

There has been very little work on the fatigue properties of rich  $\beta$ -Ti alloys. In general, the fineness of the microstructure suggests that the FC resistance will not be particularly good and will be relatively insensitive to microstructure. The smooth bar fatigue strength should be quite good, however, because of the high yield strengths that can be achieved. Here again, however, little data is available.

Table II: Typical Properties of Several  $\beta$ -Ti Alloys

<u>Alloy</u>	<u>Microstructure</u>	<u>UTS</u> <u>MPa(ksi)</u>	<u>RA</u> <u>%</u>	<u>K<sub>Q</sub></u> <u>MPa<math>\sqrt{m}</math></u>
Ti-10Mo-6Cr-3Al (Ref. 81,98)	Stringered $\alpha$ , semi-continuous GB $\alpha$ , $\alpha+\beta$ aged matrix	1330(193)	15	92
	Continuous GB $\alpha$ , $\alpha+\beta$ aged matrix	1185(172)	14	64
Ti-6.5Mo-4Cr-2.5Al (Ref. 89-98)	Stringered $\alpha$ , no GB $\alpha$ , aged $\alpha+\beta$ matrix	1240(180)	24	65
	Continuous GB $\alpha$ , aged $\alpha+\beta$ matrix	1305(189)	5	63
Ti-8Mo-8V-2Fe-3Al (Ref. 94)	GB $\alpha$ , aged $\alpha+\beta$ matrix	1255(182)	2	56
Ti-3Al-8V-6Cr- 4Zr-4Mo (Ref. 88)	GB $\alpha$ , aged $\alpha+\beta$ matrix	1450(210)	7	~42



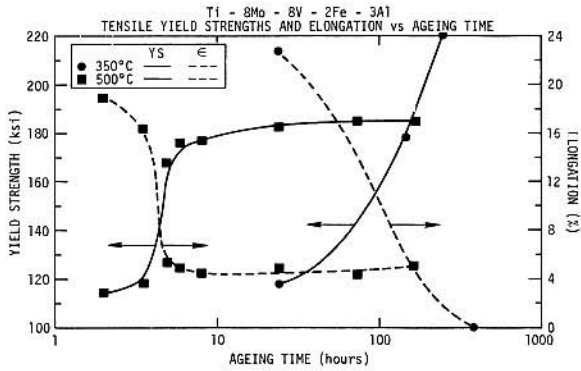


Figure 29. Yield stress and tensile elongation vs. aging time curves for Ti-8V-8Mo-2Fe-3Al aged in the uniform  $\alpha$  nucleation and sympathetic  $\alpha$  nucleation regimes (500 and 350°C, respectively).

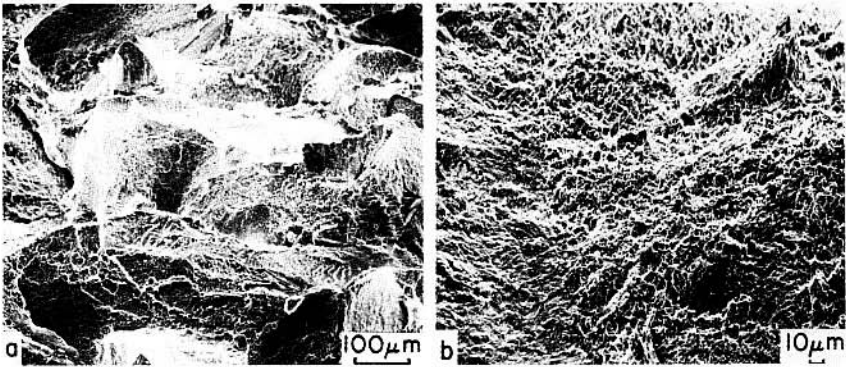


Figure 30. SEM fractographs showing the variation in fracture mode when g.b.  $\alpha$  is present or absent. a)  $\beta$ -processed, grain boundary  $\alpha$  present, b)  $\alpha+\beta$  processed, no grain boundary  $\alpha$ .

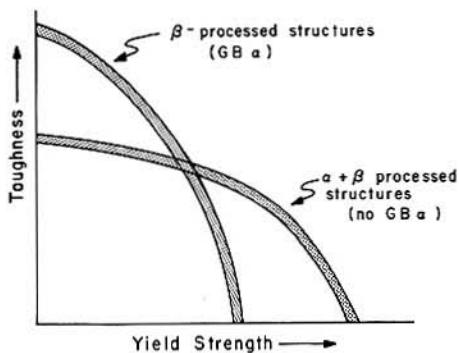


Figure 31. Schematic representation of strength-toughness trend data for  $\beta$  and  $\alpha+\beta$ -processed alloys with and without g.b.  $\alpha$ , respectively.

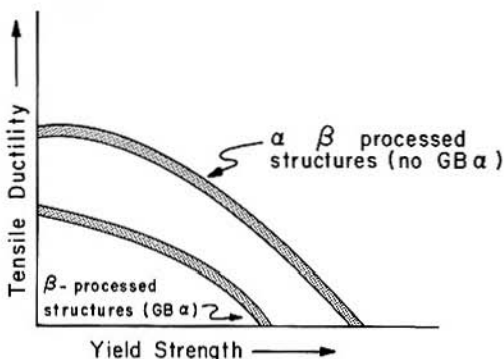


Figure 32. Schematic representation of strength-tensile ductility trend data for  $\beta$  and  $\alpha+\beta$ -processed alloys with and without grain boundary  $\alpha$ .

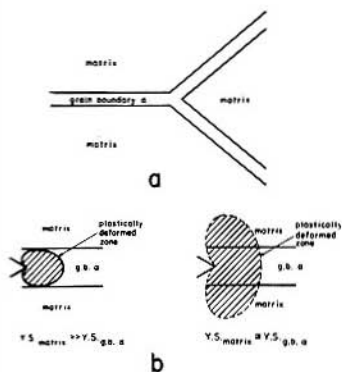


Figure 33. Schematic drawing showing how g.b.  $\alpha$  and matrix yield strength work together to affect the shape and size of the crack tip plastic zone.  
 a) schematic of microstructure  
 b) schematic of crack tip plastic zone and microstructure.

#### 4.0 Outlook for $\beta$ -Ti Alloys

The previous sections have provided a fairly complete description of the current state-of-the-art in  $\beta$ -Ti alloys. It is also appropriate to make a few comments on the most likely future applications of this class of alloys.

It is fair to say that, while  $\beta$ -Ti alloys have been around for a long time, there have been only a few instances where they have been used in any significant quantities. One reason for this is the cost of earlier  $\beta$ -Ti alloys. Another is that earlier, older alloys such as Ti-13V-11Cr-3Al have not been very producible (this is not completely independent of cost). While the current situation is somewhat better, only three alloys have been produced in any significant quantity as of the end of 1983. These are Ti-10V-2Fe-3Al, Ti-3Al-8V-6Cr-4Zr-4Mo and Ti-15V-3Cr-3Sn-3Al. The latter of these is a relatively new alloy which shows promise for excellent producibility as sheet. Other alloys such as Ti-11.5Mo-6Sn-4Zr ( $\beta$ -III) have been well-received by the engineering community, but have not actually found many applications because only one producer has shown a willingness to melt this alloy. Thus the remainder of this section will focus on pending applications of the three alloys identified earlier and some possible applications which utilize the novel physical properties of  $\beta$ -Ti alloys.

For structural applications,  $\beta$ -Ti alloys are attractive from a density corrected standpoint, especially when their generally superior resistance to stress corrosion and hydrogen embrittlement are taken into consideration. These latter factors effectively limit the strength level at which the high strength steels can be used in adverse environments. This creates a number of applications for  $\beta$ -Ti alloys. However, the increasing trend toward the use of damage tolerant design concepts also places stringent requirements on fracture-related properties such as toughness and fatigue crack propagation. As has been discussed, neither of these properties are outstanding in  $\beta$ -Ti alloys, although toughness can be manipulated by microstructural control. Since the critical flaw size is proportional to  $(K_{IC}/YS)^2$ , the toughness at strength levels of 1200 MPa (175 ksi) can be a limiting factor. The role of grain boundary  $\alpha$  in limiting the toughness of  $\beta$ -Ti alloys means that constant additional care must be utilized in processing these alloys. It is easier to process the lean  $\beta$ -Ti alloys to avoid grain boundary  $\alpha$ , but for heavy section applications, the lean  $\beta$ -Ti alloys are less hardenable. Moreover, there generally are more situations that are limited by fatigue than by toughness, thus the relative insensitivity of FCP resistance of  $\beta$ -Ti alloys is especially troublesome.

For very high strength applications such as fasteners and springs, the rich  $\beta$ -Ti alloys are attractive because they can be cold reduced after  $\beta$ -solution treatment then formed and aged to very high strength levels. The somewhat lower modulus of these alloys coupled with their very high yield strength permits a large elastic deflection range in springs made of these alloys. In alloys which exhibit stress-assisted martensite, the superelastic behavior is also attractive but has not been utilized to any extent yet.

The other novel properties of  $\beta$ -Ti alloys such as shape memory effect also offer a number of interesting potential applications, but only time can permit determination of the extent to which this will be utilized.

In summary, the  $\beta$ -Ti alloys may be on the threshold of an era of increased utilization, but the constraints of cost and producibility coupled with the somewhat lower fracture-related properties will require continued attention. In the final analysis, the emergence of new structures which provide improved efficiency may require the simultaneous re-examination of the

constraints placed on materials by the conservative designs dictated by damage tolerant criteria.

#### 5.0 Acknowledgments

The authors thank several of their colleagues for helpful discussions and for reading and commenting on this manuscript. In particular, J. E. Costa and D. Banerjee. We also express our gratitude to Mrs. A. M. Crelli and M. Glatz for their assistance in preparing the photo-ready manuscript. One of us (J.C.W.) also acknowledges the support of the Office of Naval Research. We also acknowledge use in this paper of unpublished results of joint research by J. C. Williams and C. G. Rhodes.

## 6.0 References

1. J. Goldberg and C. Burstone, J. Dent. Res., 58, 593 (1979).
2. R. R. Boyer and R. Bajoraitis, "Ti-3Al-8V-4Mo-4Zr Wire for Spring Applications," paper presented at TMS-AIME Annual Meeting, Atlanta, GA, March 1983.
3. A. M. Sherman, "Torsional Properties and Performance of Beta Titanium Alloy Springs," paper presented at TMS-AIME Annual Meeting, Atlanta, GA, March 1983.
4. E. W. Collings, "Titanium-Niobium Alloy Superconductors," paper presented at TMS-AIME Annual Meeting, Atlanta, GA, March 1983.
5. E. M. Savitskiy, M. I. Bychkova, and V. V. Baron, "Structure Characteristics and Superconducting Properties of Ti-Nb Alloys," p. 735 in Titanium '80 Science and Technology, H. Kimura and O. Izumi, eds.; AIME, New York, NY, 1980.
6. T. W. Duerig, D. F. Richter, and J. Albrecht, Scripta Met., 16, 957 (1982).
7. C. Baker, Met. Sci. J., 175 (6) (1972).
8. T. W. Duerig and G. Schroeder, Brown-Boveri Report: KLR 82-147 B, September 1982.
9. G. W. Kuhlman and T. B. Gurganus, Met. Prog., p. 30 (1980).
10. T. W. Duerig, G. T. Terlinde, and J. C. Williams, Metall. Trans., 11A, (1980), p. 1987.
11. C. C. Chen, J. A. Hall, R. R. Boyer, p. 457, Titanium '80 Science and Technology, H. Kimura and O. Izumi, eds.; AIME, New York, NY, 1980.
12. F. H. Froes, et al., (in this volume).
13. R. R. Boyer, J. of Metals, p. 61 (1980).
14. T. W. Duerig, Ph.D. Thesis, Carnegie-Mellon University, 1980.
15. F. A. Crossley and W. J. Garice, J. of Metals, p. 26 (Feb. 1981).
16. T. W. Duerig, G. T. Terlinde, and J. C. Williams, "The Omega Phase Reaction in Titanium Alloys," p. 1299 in Titanium '80 Science and Technology, H. Kimura and O. Izumi, eds.; AIME, New York, NY, 1980.
17. M. J. Blackburn and J. C. Williams, Trans. AIME, 242, (1968), p. 813.
18. S. L. Sass, Acta Met., 17, 813 (1969).
19. D. De Fontaine, N. E. Paton, and J. C. Williams, Acta Met., 19, 1153 (1971).
20. H. E. Cook, Acta Met., 23, 1041 (1975).
21. B. S. Hickman, J. Mat. Sci., 554 (21) (1969).

22. J. Jamieson, Science, **140**, 72 (1963).
23. T. W. Duerig, J. Albrecht, D. Richter, and P. Fischer, Acta Met., **30**, 2161 (1982).
24. T. W. Duerig, G. T. Terlinde, R. Middleton, and J. C. Williams, "Stress Assisted Transformation in Ti-10-2-3," p. 1503 in Titanium '80 Science and Technology, H. Kimura and O. Izumi, eds.; AIME, New York, NY, 1980.
25. H. Sasano, T. Suzuki, O. Nakano, and H. Kimura, "Crystal Structure of Martensites," p. 717 in Titanium '80 Science and Technology, H. Kimura and O. Izumi, eds.; AIME, New York, NY, 1980.
26. J. C. Williams, "Critical Review - Kinetics and Phase Transformations," Titanium Science and Technology, R. I. Jaffee and H. M. Burte, eds.; **3**, 1433 (1972).
27. H. M. Flower, R. Davis, and D.R.F. West, "Martensite Formation and Decomposition in Alloys of Titanium Containing Beta Stabilization Elements," p. 1703 in Titanium and Titanium Alloys, J. C. Williams and A. F. Belov, eds.; Plenum Press, New York, NY, 1982.
28. R. Davis, H. M. Flower, and D.R.F. West, J. Mat. Sci., 712 (14) (1979).
29. C. Hammond, Scripta Met., **6**, 569 (1972).
30. R. Coade, T. W. Duerig, and G. H. Gessinger, "Effect of Microstructure on the Mechanical Properties of Transage 134," p. 263 in Strength of Metals and Alloys, R. C. Gifkins, ed., (1982).
31. C. G. Rhodes and J. C. Williams, unpublished research, Rockwell Science Center, 1972.
32. R. A. Spurling, C. G. Rhodes, and J. C. Williams, Metall. Trans., **5A**, (1974), p. 2597.
33. G. M. Pennock, H. M. Flower, and D.R.F. West, Metallography **10** 43, (1977).
34. R. M. Middleton and C. R. Hickey, Jr., "Transformation Characteristics of Transage Titanium 129," p. 1567 in Titanium and Titanium Alloys, J. C. Williams and A. F. Belov, eds.; Plenum Press, New York, NY, 1982.
35. T. W. Duerig and J. Gould, unpublished research (1982).
36. J. R. Toran and R. R. Biederman, "Phase Transformation Study of Ti-10V-2Fe-3Al," p. 1491 in Titanium '80 Science and Technology, H. Kimura and O. Izumi, eds.; AIME, New York, NY, 1980.
37. F. A. Crossley and R. W. Lindberg, "Microstructural Analysis of a High Strength Martensite Beta Titanium Alloy," Proceedings of the 2nd Int. Conf. on the Strength of Metals and Alloys, Vol. III, p. 841, ASM, 1970.
38. F. A. Crossley, "Fracture Toughness of Transage 129 Alloy, Ti-2Al-11V-2Sn-11Zr," p. 2025 in Titanium Science and Technology, R. I. Jaffee and H. M. Burte, eds.; Plenum Press, New York, NY, 1972.
39. F. A. Crossley, "Three Heat Treatment Paths to 120MPa or Greater Strength in Transage 134 Martensitic Titanium Alloy," paper presented at TMS-AIME Annual Meeting, Dallas, TX, February 1982.

40. R. W. Coade and T. W. Duerig, "A Survey of the Beta Titanium Alloy, Transage 134," Brown-Boveri Report KLR 82-157 C, September 1982.
41. S. Niyazaki, K. Otsuka, and Y. Suzuki, Scripta Met., 15, 287 (1981).
42. N. E. Paton and J. C. Williams, "The Deformation of Body-Centered-Cubic Titanium-Vanadium Single Crystals," Proceedings of Second International Conf. on Strength of Metals and Alloys, Vol. 1, p. 108, ASM (1970).
43. M. Oka and Y. Taniguchi, Metall. Trans., 10A, (1979), p. 651.
44. A. P. Young, R. I. Jaffee, and C. M. Schwartz, Acta Met., 11, 1097 (1963).
45. M. J. Blackburn and J. A. Feeney, J. Inst. Metals, 99, 132 (1971).
46. H. G. Paris, B. G. LeFevre, and E. A. Starke, Metall. Trans., 7A, (1976), p. 273.
47. C. M. Wayman and K. Shimizu, Met. Sci. J., 6, 175 (1972).
48. L. Delaey, R. V. Krishnan, H. Tas, and H. Warlimont, J. Mat. Sci., 1521 (9) (1974).
49. Y. Z. Vintaykin, Y. G. Virakhovskiy, I. Y. Georgiyeva, Y. B. Gurevich, V. B. Dnitriyev, D. F. Litvin, and V. A. Udovenko, Phys. Met. Metall., Vol. 45, p. 170 (1979).
50. M. J. Blackburn and J. C. Williams, Trans. Met. Soc. AIME, 242, (1968), p. 2461.
51. M. K. Koul and J. F. Breedis, Acta Met., 18, 579 (1970).
52. A.I.P. Nwobu, "Decomposition of Beta Phase in Transage 134 and 129 Titanium Alloys," Master's Thesis, Imperial College, London, 1979.
53. M. J. Feeney and M. J. Blackburn, Metall. Trans., 1, (1976), p. 3309.
54. T. Nishimura, M. Nishigaki, and S. Ohtani, J. Japan Inst. Met., 40, 219 (1976).
55. E.S.K. Menon and R. Krishnan, J. Mat. Sci., 375 (18) (1983).
56. B. S. Hickman, Trans. Met. Soc. AIME, 245 (1969), p. 1329.
57. C. Hammond and J. Nutting, Metal Science, p. 474 (1977).
58. J. C. Williams and M. J. Blackburn, Trans. Met. Soc. AIME, 245, (1969), p. 1329.
59. J. C. Williams, B. S. Hickman, and H. L. Marcus, Metall. Trans., 2, (1971), p. 1913.
60. A. Bowen, "Omega in Beta Alloys," (in this volume).
61. Y. Murakami, "Phase Transformation and Heat Treatment," p. 153 in Titanium '80 Science and Technology, H. Kimura and O. Izumi, eds.; AIME, New York, NY, 1980.

62. C. G. Rhodes and J. C. Williams, Metall. Trans., 6A, 2103 (1975).
63. D. Banerjee and J. C. Williams, unpublished research, Carnegie-Mellon University (1983).
64. J. C. Williams and M. J. Blackburn, J. Quart. Trans. ASM, 60, 373 (1967).
65. G. M. Pennock, H. M. Flower, and D.R.F. West, "The Control of  $\alpha$  Precipitation by Two Step Ageing in  $\beta$  Ti-15%Mo," p. 1343 in Titanium '80 Science and Technology, H. Kimura and O. Izumi, eds.; AIME, New York, NY, 1980.
66. J. C. Williams and M. J. Blackburn, Trans. AIME, 245, 2352 (1969).
67. T. Nishimura, M. Nishigaki, and H. Kusamichi, "Ageing Characteristics of Beta Titanium Alloys," p. 1675 in Titanium and Titanium Alloys, J. C. Williams and A. F. Belov, eds.; Plenum Press, New York, NY, 1982.
68. M. A. Nikhanovov and V. V. Latsh, "Transformation in Unstable Beta Titanium Alloys," p. 1651 in Titanium and Titanium Alloys, J. C. Williams and A. F. Belov, eds.; Plenum Press, New York, NY, 1982.
69. M. G. Mendiratta, G. Luetjering, and S. Weissman, Metall. Trans., 2, 2599 (1971).
70. J. C. Williams, F. H. Froes, C. F. Yolton, and I. M. Bernstein, "The Influence of TMP on the Microstructure of Metastable  $\beta$ -Ti Alloys," p. 639 in Titanium and Titanium Alloys, J. C. Williams and A. F. Belov, eds.; Plenum Press, New York, NY, 1982.
71. M. J. Blackburn, Quart. Trans. ASM, 59, 694 (1966).
72. R. Davis, H. M. Flowers, and D.R.F. West, Acta Met., 27, 1041 (1971).
73. I. A. Bagariatskii, G. I. Nosava, and T. V. Tagunova, Soviet Phys. Doklady, 3, 1014 (1959).
74. H. I. Aaronson, p. 481, in Decomposition of Austenite by Diffusional Processes, V. F. Zackay and H. I. Aaronson, eds.; Interscience, New York, 1962.
75. F. H. Froes, J. C. Chesnutt, C. G. Rhodes, and J. C. Williams, "Relationship of Fracture Toughness and Ductility to Microstructure and Fractographic Features in Advanced Deep Hardenable Ti Alloys," ASTM Symposium Fracture Toughness of Titanium Alloys, Toronto, 1977.
76. G. Terlinde, T. W. Duerig, and J. C. Williams, Metall. Trans., 14A, 2101 (1983).
77. J. B. Guernsey, V. C. Petersen, and E. J. Dulis, Metal Progress, 96, 121 (1969).
78. F. A. Crossley and J. M. Van Orden, Met. Eng. Quart., 13, 55 (May 1973).
79. A. Gysler, G. Luetjering, and V. Gerold, Acta Met., 22, 901 (1974).
80. A. Gysler, G. T. Terlinde, and G. Luetjering, "Influence of Grain Size on the Ductility of Age-Hardenable Titanium Alloys," p. 1919 in Titanium and Titanium Alloys, J. C. Williams and A. F. Belov, eds.; Plenum Press, NY, 1982.



81. R. R. Boyer, "Metallurgical Evaluation and Design Properties of High Strength Ti-10-2-3 Forging," paper presented at TMS-AIME Fall Meeting, Milwaukee, WI, 1979.
82. K. S. Chan, C. C. Wojcik, D. A. Koss, Metall. Trans., 12A, 1899 (1981).
83. M. Young, E. Levine, and H. Margolin, Metall. Trans., 10A, 359 (1979).
84. T. Hamajima, G. Luetjering, and S. Wiessman, Metall. Trans., 4, 847 (1973).
85. J. C. Chesnutt and F. H. Froes, Metall. Trans., 8A, 1013 (1977).
86. P. P. Bonsel and A. J. Ardell, Metallography, 5, 97 (1972).
87. J. P. Simpson and E. Toeroek, "Dynamic Elastic and Damping Properties of Some Practical Ti-Base Alloys," p. 601 in Titanium '80 Science and Technology, H. Kimura and O. Izumi, eds.; AIME, New York, NY, 1980.
88. H. J. Rack, "Strength/Fracture Toughness Relationships in Aged Ti-3Al-8V-6Cr-4Mo-4Zr," p. 1627 in Titanium '80 Science and Technology, H. Kimura and O. Izumi, eds.; AIME, New York, NY, 1980.
89. F. H. Froes, J. C. Chesnutt, C. G. Rhodes, and J. C. Williams, "Relationship of Fracture Toughness and Ductility to Microstructure and Fractographic Features in Advanced Deep Hardenable Titanium Alloys," ASTM STP (1977).
90. J. E. Coyne, "The Beta Forging of Titanium Alloys," p. 97 in Titanium '80 Science and Technology, H. Kimura and O. Izumi, eds.; AIME, New York, NY, 1980.
91. R.J.H. Wanhill, J. Inst. Metals, 101, 258 (1973).
92. I. W. Hall and C. Hammond, p. 1365, 2nd International Conference on Ti and Ti-Alloys, Boston, MA, 1976.
93. J. A. Hall, C. M. Pierce, D. L. Ruckle, and R. A. Sprague, "Property-Microstructural Relationships in the Ti-6Al-2Sn-4Zr Alloy," Air Force Report AFML-TR-71-206 (1971).
94. R. Chait and T. S. DeSisto, "The Fracture Toughness of 3 Ti Alloys," p. 1377 in Titanium Science and Technology, R. I. Jaffee and H. M. Burte, eds.; Plenum Press, New York, 1973.
95. G. M. Ludtka, Ph.D. Thesis, Carnegie-Mellon University, (1981).
96. M. A. Greenfield and H. Margolin, Metall. Trans., 2, 841 (1971).
97. T. W. Duerig, J. E. Allison, and J. C. Williams, "Fatigue Crack Growth Rates in Ti-10-2-3," submitted to Metall. Trans. (1983).
98. J. C. Williams, F. H. Froes, J. C. Chesnutt, C. G. Rhodes, and R. G. Berryman, ASTM STP 651, Philadelphia, PA (1978).
99. W. C. Leslie, The Physical Metallurgy of Steels, p. 294, McGraw-Hill, New York, 1981.
100. R. C. Garvie, R. H. Hannink, and R. T. Pascoe, Nature 258, 703 (1975).

101. J. Albrecht, T. W. Duerig, and D. Richter, "Mechanical Properties Solution Treated and Quenched Ti-10-2-3," paper presented at TMS-AIME Annual Meeting, Dallas, TX, 1982.
102. F. A. Crossley, J. of Aircraft, 18, 993 (1981).
103. S. B. Chakraborty, T. K. Mukhopadhyay, and E. A. Starke, Acta Met., 26, 909 (1979).
104. S. B. Chakraborty and E. A. Starke, Metall. Trans., 10A, 1901 (1979).
105. M. O. Speidel, High Temperature Materials in Gas Turbines, p. 207, P. R. Sahm and M. O. Speidel, eds., New York, NY (1974).
106. E. Hornbogen and K. H. Zum Gahr, Acta Met., 24, 581 (1976).
107. A. Gysler, J. Lindigkeit, and G. Luetjering, "Correlation Between Microstructure and Fatigue Fracture," Proc. of 5th Int. Conference on the Strength of Metals and Alloys 2, 1113, (1979).
108. J. C. Williams and G. Luetjering, "The Effect of Slip Length and Slip Character on the Properties of Titanium Alloys," p. 671 in Titanium and Titanium Alloys, J. C. Williams and A. F. Belov, eds.; Plenum Press, NY, 1982.
109. E. Hornbogen, Acta Met., 26, 147 (1978).
110. A. Gysler, G. Luetjering, and V. Gerold, Acta Met., 22, 901 (1974).
111. G. T. Terlinde and J. C. Williams, unpublished research.
112. C. G. Rhodes and J. C. Williams, unpublished research, Rockwell International, 1972.
113. J. C. Williams and E. A. Starke, Jr., "The Role of Thermomechanical Processing in Tailoring the Properties of Aluminum and Titanium Alloys," ASM Seminar Series, G. Krauss, ed. (in press).